NWC TP 6953

Noise and False Alarm Rate Characteristics for Envelope Detector Systems Preceded by RF Amplification

by
Brad Wiitala
Attack Weapons Department

NOVEMBER 1988

NAVAL WEAPONS CENTER
CHINA LAKE, CA 93555-6001

Naval Weapons Center

FOREWORD (U)

The investigation described in this report was performed at the Naval Weapons Center during August 1986 through May 1988. The work was authorized by the Naval Air systems Command under AIRTASK A540-5402/008-F/8W18070000.

This report was reviewed for technical accuracy by Richard Smith Hughes.

Approved by
P. B. HOMER, *Head*
Attack Weapons Department
28 September 1988

Under authority of
J. A. BURT
Capt., U.S. Navy
Commander

Released for publication by
G. R. SCHIEFER
Technical Director

NWC Technical Publication 6953

Published by .... Technical Information Department
Collation .... Cover, 23 leaves
First printing .... 68 copies

UNCLASSIFIED

SECURITY CLASSIFICATION OF THIS PAGE (*When Data Entered*)

REPORT DOCUMENTATION PAGE

1a REPORT SECURITY CLASSIFICATION UNCLASSIFIED	1b RESTRICTIVE MARKINGS
2a SECURITY CLASSIFICATION AUTHORITY	3 DISTRIBUTION/AVAILABILITY OF REPORT "A" statement
2b DECLASSIFICATION/DOWNGRADING SCHEDULE	
4 PERFORMING ORGANIZATION REPORT NUMBER(S) NWC TP 6953	5 MONITORING ORGANIZATION REPORT NUMBER(S)
6a NAME OF PERFORMING ORGANIZATION Naval Weapons Center 6b OFFICE SYMBOL (If Applicable)	7a NAME OF MONITORING ORGANIZATION
6c ADDRESS (City, State, and ZIP Code) China Lake, CA 93555-6001	7b ADDRESS (City, State, and ZIP Code)
8a NAME OF FUNDING/SPONSORING ORGANIZATION NAVAIR 8b OFFICE SYMBOL (If Applicable)	9 PROCUREMENT INSTRUMENT IDENTIFICATION NUMBER AIRTASK A540-5402/008-F/8W18070000
8c Address (City, State, and ZIP Code) AIR-5402 Washington, D.C. 20360-5402	10 SOURCE OF FUNDING NUMBERS PROGRAM ELEMENT NO | PROJECT NO | TASK NO (SEE COLUMN 9) | WORK UNIT NO

11 TITLE (Include Security Classification)

NOISE AND FALSE ALARM RATE CHARACTERISTICS FOR ENVELOPE DETECTOR SYSTEMS PRECEDED BY RF AMPLIFICATION (U)

12 PERSONAL AUTHOR(S)

Wiitala, Brad

13a TYPE OF REPORT	13b TIME COVERED	14 DATE OF REPORT (Year, Month, Day)	15 PAGE COUNT
Final	*From* 86 Aug *To* 88 May	1988, November	44

16 SUPPLEMENTARY NOTATION

17 COSATI CODES

FIELD	GROUP	SUB-GROUP

18 SUBJECT TERMS (Continue on reverse side if necessary and identify by block number)

Noise Characteristics
False Alarm Rate
Envelope Detector Systems
Video Amplification
Following Detector
Crest Factor

19 ABSTRACT (Continue on reverse side if necessary and identify by block number)

(U) The noise and false alarm rate (FAR) characteristics at the video output of square-law envelope-detector systems preceded by RF amplification are explored. The analysis is presented from a "crest factor" point of view; i.e., the relationship between the peaks and root-mean-square (RMS) levels of the noise present at the video output. This relationship should be especially useful for those working with FAR statistics if one explores the following question: Given an RMS level of noise, what is the signal threshold voltage necessary to produce the desired FAR at the threshold detector output? No attempt is made to actually formulate an equation to predict

(Contd. on back)

20 DISTRIBUTION/AVAILABILITY OF ABSTRACT	21 ABSTRACT SECURITY CLASSIFICATION
☒ UNCLASSIFIED/UNLIMITED ☐ SAME AS RPT. ☐ DTIC USERS	Unclassified

22a NAME OF RESPONSIBLE INDIVIDUAL	22b TELEPHONE (Include Area Code)	22c OFFICE SYMBOL
Brad Wiitala	(619) 939-2982	NWC Code 3524

DD FORM 1473, 84 MAR

83 APR edition may be used until exhausted.
All other editions are obsolete.

SECURITY CLASSIFICATION OF THIS PAGE

UNCLASSIFIED

19. (Contd.)

the threshold voltage necessary for a given FAR and receiver configuration. Instead, an attempt is made through discussion and test data to give the reader an understanding of how the video noise changes in nature when the receiver contributes noise at the video output.

Accession For	
NTIS GRA&I	☒
DTIC TAB	☐
Unannounced	☐
Justification	
By	
Distribution/	
Availability Codes	
Dist	Avail and/or Special
A-1	

DEPARTMENT OF THE NAVY
NAVAL WEAPONS CENTER
CHINA LAKE CALIFORNIA 93555 6001

IN REPLY REFER TO
5600
341/Ser 15911
13 December 1988

From: Commander, Naval Weapons Center

Subj: ERRATA FOR NWC TECHNICAL PUBLICATION 6953, NOISE AND FALSE ALARM RATE CHARACTERISTICS FOR ENVELOPE DETECTOR SYSTEMS PRECEDED BY RF AMPLIFICATION, dtd November 1988

1. Please make the following pen and ink changes on the subject report:

   a. Page 41, Figure B-3, change Positive-Going Noise Pulse of Gaussian-Distributed Noise to Negative-Going Noise Pulse of Gussian-Distributed Noise.

   b. Page 41, Figure B-4, Change Negative-Going Noise Pulse of Rayleigh-Distributed Noise to Positive-Going Noise Pulse of Rayleigh-Distributed Noise.

   c. Page 42, Figure B-5, change Positive-Going Noise Pulse of Rayleigh-Distributed Noise to Negative-Going Noise Pulse of Rayleigh-Distributed Noise.

B. W. Butler
B. W. BUTLER
By direction

Distribution:

2 Naval Air Systems Command (AIR-5004)
2 Naval Sea Systems Command (SEA-09B312)
1 Commander in Chief, U. S. Pacific Fleet, Pearl Harbor (Code 325)
1 Commander, Third Fleet, San Francisco
1 Commander, Seventh Fleet, San Francisco
2 Naval Academy, Annapolis (Director of Research)
1 Naval War College, Newport
1 Air Force Intelligence Agency, Bolling Air Force Base (AFIA/INTAW, MAJ R. Esaw)
12 Defense Technical Information Center, Alexandria
1 American Electronic Laboratories, Incorporated, Lansdale, PA (J. Wadkowski)
2 California Microwave, Incorporated, Sunnyvale, CA
   R. Hardy (1)
   J. Hettinger (1)
3 Ford Aerospace and Communications Corporation, Newport Beach, CA
   S. Carruth (1)
   P. Juul (1)
   J. Possi (1)
1 Hudson Institute, Incorporated, Center for Naval Analyses, Alexandria, VA (Technical Library)

CONTENTS

Tables:

INTRODUCTION

This report explores the noise and false alarm rate (FAR) characteristics at the video output of square-law envelope-detector systems preceded by RF amplification. The analysis is presented from a "crest factor" point of view; i.e., the relationship between the peaks and root-mean-square (RMS) levels of the noise present at the video output. This relationship should be especially useful for those working with FAR statistics if one explores the following question: Given an RMS level of noise, what is the signal threshold voltage necessary to produce the desired FAR at the threshold detector output?

Two types of noise are present in the envelope detector system described above. The first type is the noise contributed by the detector and video amplifiers. This type of noise is present at the video output with no RF amplification and is primarily Gaussian in nature. The second type of noise present is that contributed by the RF electronics, such as mixers, local oscillators (LOs), and RF amplifiers. The characteristics of this type of noise can be considerably different than those of the first type because the noise is essentially detected receiver noise. The detected receiver noise characteristics are primarily determined by several variables: the transfer function of the detector (square-law or linear), the RF bandwidth, and the video bandwidth.

This report will also cover two types of video amplification following the detector. The first type is simple linear amplification. This discussion will give the reader some valuable insight into what happens to the video output noise characteristics when the receiver noise passes through the detector. The second type of video amplification considered is logarithmic amplification. Logarithmic amplification will be considered because logarithmic amplifiers are widely used as compressive elements in radar and electronic warfare (EW) receivers.

No attempt is made to actually formulate an equation to predict the threshold voltage necessary for a given FAR and receiver configuration. Instead, an attempt is made through discussion and test data to give the reader an understanding of how the video noise changes in nature when the receiver contributes noise at the video output.

THRESHOLD DETECTION SYSTEM

Threshold detection is used because of the real-time considerations necessary for an EW or radar receiver system. Once a threshold indication is given, signal processing takes place immediately. For example, if the radar pulse is very narrow, the pulse may have to be "captured" by follow-and-hold action before it can be digitized by an analog-to-digital (A/D) converter.

The proper threshold voltage is a compromise in sensitivity between the importance either of the circuit failing to recognize a signal that is present or to falsely indicate the presence of a signal when none exists. This latter situation is referred to as a false alarm detection. To achieve the best sensitivity possible for a given system, the FAR must be set as high as possible. This setting is minimally an order of magnitude less than the minimum signal pulse repetition frequency (PRF). The tradeoffs between too high and too low a signal threshold voltage can be summarized as follows:

1. Signal threshold voltage set too high;

   a. Loss of sensitivity.

   b. Loss of dynamic range.

2. Signal threshold voltage set too low;

   a. Excessive FAR.

   b. Possible saturation of signal processing circuits.

Figure 1 shows a basic threshold-detection circuit. Threshold detection is based upon establishing a threshold voltage at the video output of a radar or EW receiver. If the video output exceeds the threshold voltage, a signal is assumed to be present.

Figure 2 is an oscilloscope display showing a video pulse, a signal threshold voltage level, and the output of a comparator indicating a threshold detection.

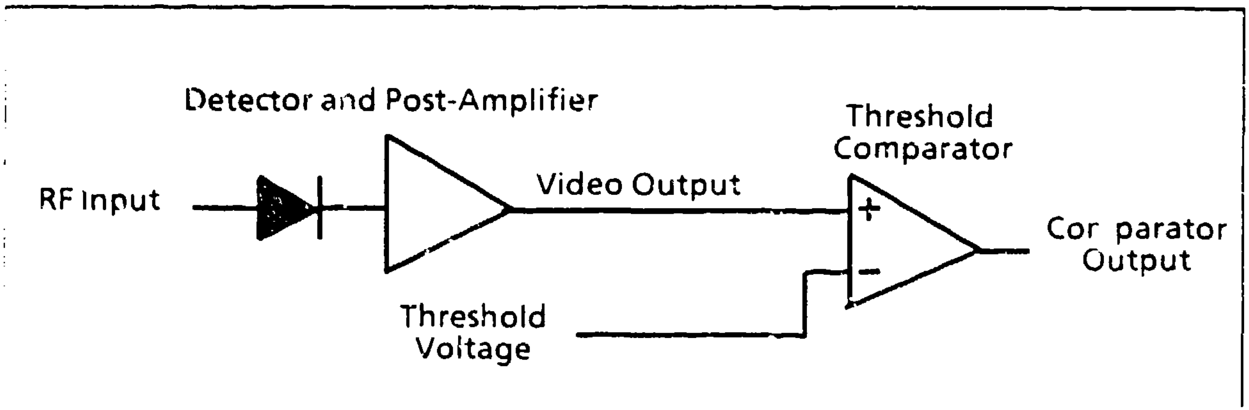

FIGURE 1. Threshold Detector Circuit.

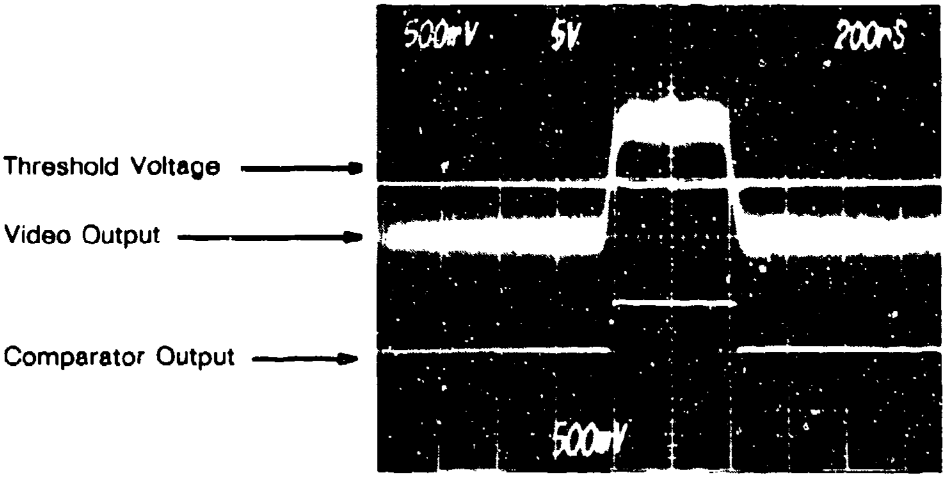

FIGURE 2. Video Output, Signal Threshold Voltage, and Comparator Output. Scale for threshold voltage and video output = 500mV/division; comparator output = 5 V/division.

SQUARE-LAW ENVELOPE DETECTION SYSTEM

Figure 3 shows an envelope detector system preceded by RF amplification. Generally, the sensitivity of the system increases with increasing RF gain, G_{RF}, until the internal RF noise, P_{NRF}, is of the same magnitude as the signal power, P_{SIG}. At this point, P_{NRF} is contributing noise at the output of the video amplifier. The nature of the noise at V_{OUT} (spectral and amplitude distribution) then changes (Reference 1).

The total noise at V_{OUT} is due to three sources:

1. The detector diode and video amplifiers (V_{NV}).
2. The detector acts as a mixer in that the receiver noise mixes with itself in the detector (P_{NRF}).
3. The mixing of the actual signal with receiver noise in the detector (P_{SIG} and P_{NRF}).

The subsequent sections discuss the nature of the noise contributed by the first two sources.

What can be gained from learning about the nature of the noise at the video output? This question can be answered more readily by looking at the sensitivity versus RF gain data of an actual envelope detector system as shown in Figure 4.

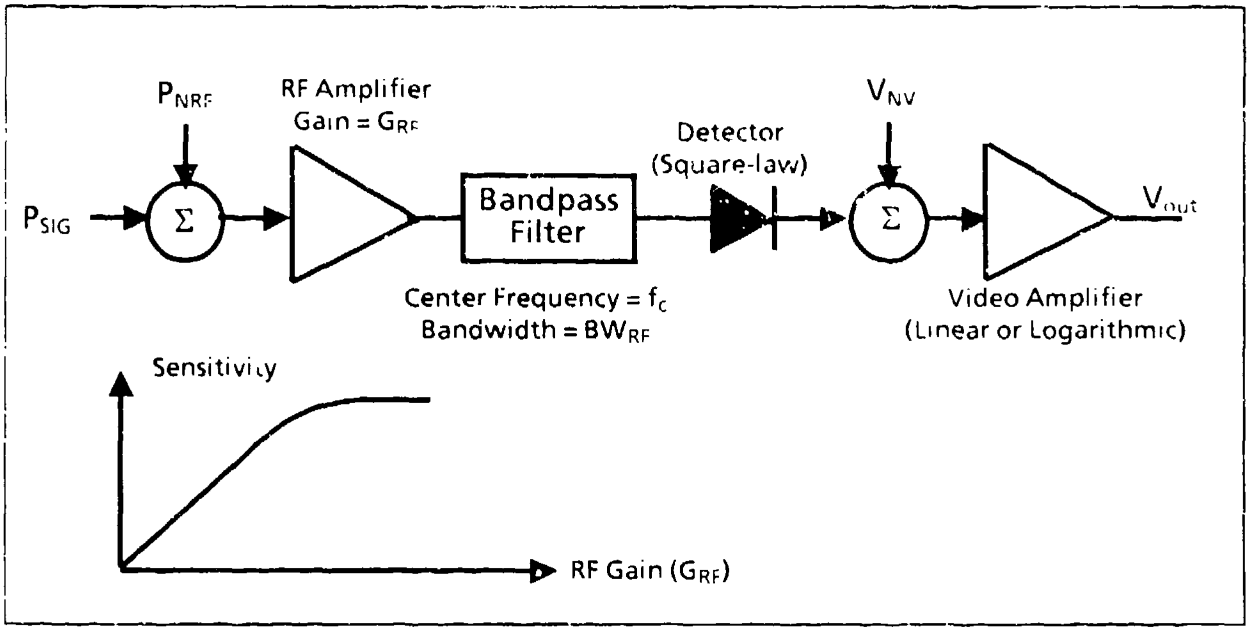

FIGURE 3. Square-Law Envelope Detector With RF Preamplification.

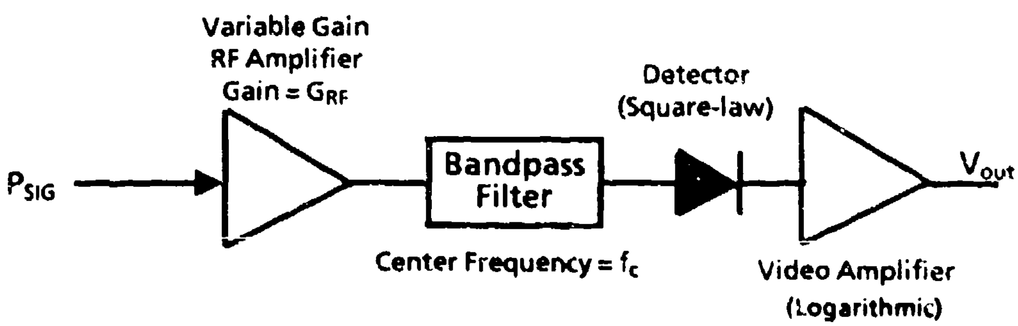

FIGURE 4. Square-Law Envelope Detector With RF Preamplification.

The characteristics of the envelope detector system used to obtain the sensitivity-versus-RF-gain test data to follow are

1. Noise figure of RF amplifier = 2.3 dB.

2. Center frequency ≫ RF bandwidth.

3. Detector type: tunnel diode.

4. Post amplification: logarithmic

5. Video bandwidth ≈ 10.0 MHz.

6. Sensitivity with no RF preamplification ≈ -38 dBm (decibels above or below 1 milliwatt).

The sensitivity-versus-RF-gain test of the Figure 4 envelope detector system was performed using the following steps:

1. Set the receiver for the desired gain.

2. With no signal input present, adjust the signal threshold voltage, V_{SIGTHR}, to give a FAR of about 100 Hz. Measure and record the FAR and V_{SIGTHR}.

3. Feed a 2-kHz, 500-ns pulse signal into the RF input and adjust the signal power level to give a comparator output count of 80% of 2 kHz (1.6 kHz). Record the power level.

4. Repeat for all gain settings.

Figures 5 and 6 are the test results of the sensitivity-versus-RF-gain test performed on the Figure 4 envelope-detector system. The test data are taken across the available gain control region in 0.5-dB increments. For each gain setting, the RMS noise level, FAR, V_{SIGTHR}, and sensitivity were recorded. The target parameters used were (1) pulse width = 500 ns; (2) PRF = 2.0 kHz.

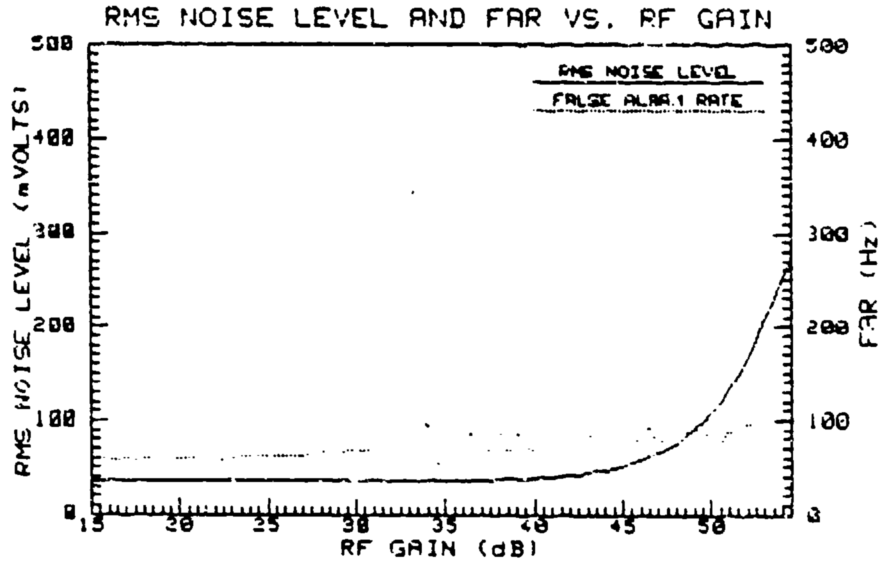

FIGURE 5. RMS Noise Level and FAR Versus RF Gain.

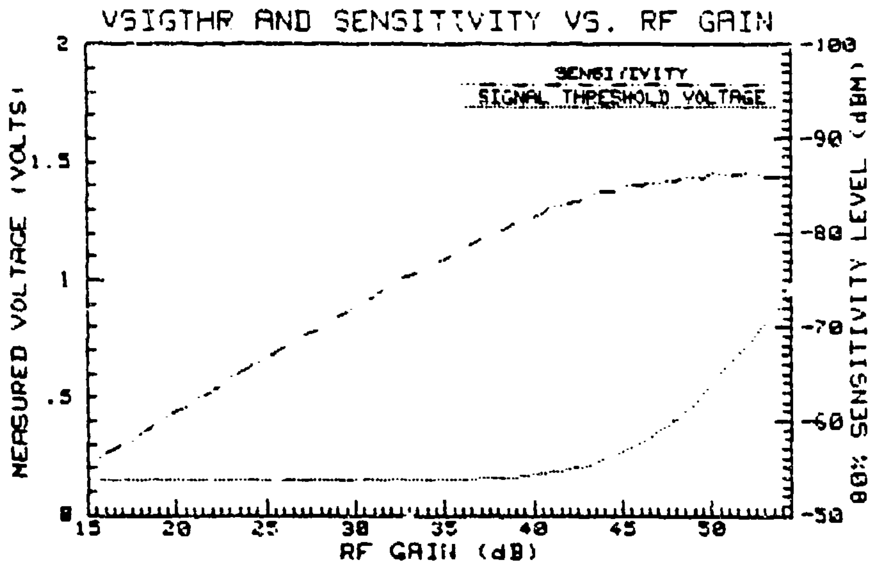

FIGURE 6. Signal Threshold Voltage and Sensitivity Versus RF Gain

ADAPTIVE SIGNAL THRESHOLD

If the system designer is trying to obtain the best sensitivity possible, the RF gain must be set at a level at which the video output noise is largely made up of noise contributed by the receiver. If the RF gain were to deviate from this gain setting due to time, temperature, or the implementation of an automatic gain control (AGC) loop, and the signal threshold voltage were fixed, two possible consequences could occur; either a loss of sensitivity in the case of decreased gain or an intolerable increase in the FAR for an increase in gain. These two problems dictate the need for some kind of adaptive signal threshold if the best sensitivity is to be gained from a given system.

Figure 7 is a proposed adaptive signal threshold circuit. The video output is fed to the input of the signal threshold comparator and the input of a device that measures the true RMS level of the noise only. The true RMS level is then multiplied by a DC gain term to set the signal threshold voltage. Under what conditions, if any, will the proposed adaptive signal threshold yield a constant FAR, and what is the value of K needed for a given type of input noise? This report will attempt to answer these two important questions.

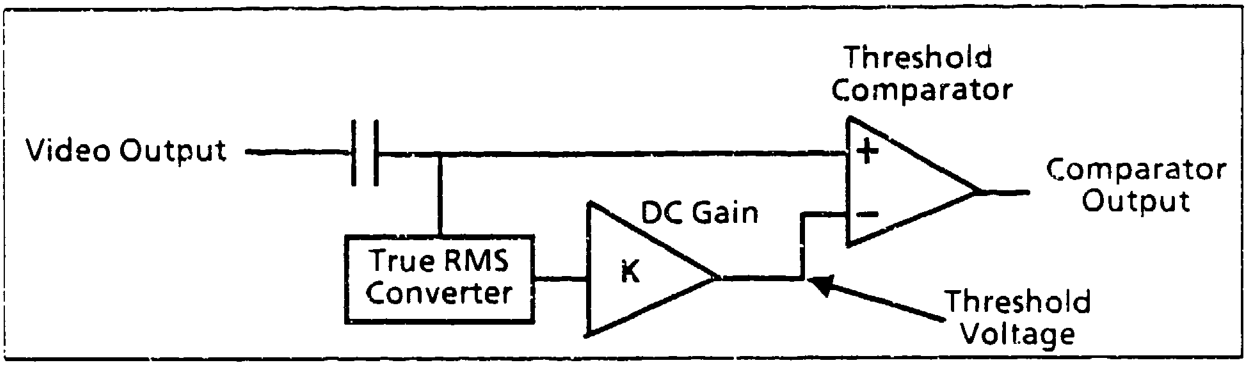

FIGURE 7. Proposed Adaptive Signal Threshold.

VIDEO OR POST-DETECTION NOISE CHARACTERISTICS

Figure 8 shows a detector stage followed by linear gain. Assuming that no signal or noise is present at the detector input, the noise at the video output is contributed solely by the detector diode and the video amplifiers. This noise is commonly referred to as video or post-detection noise.

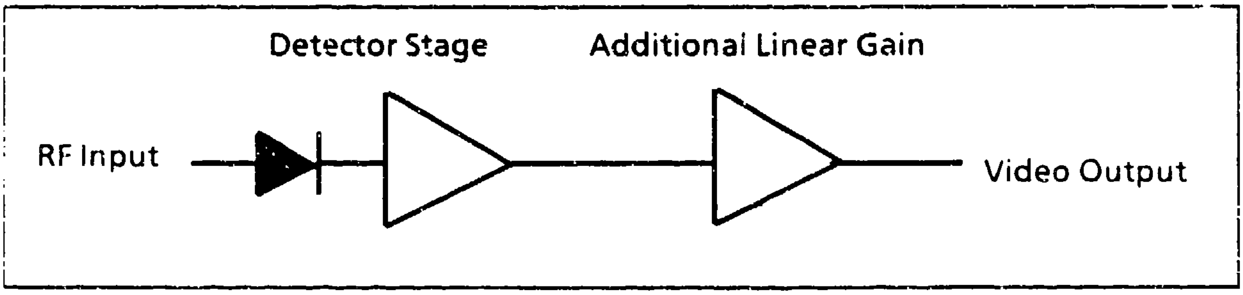

FIGURE 8. Detector Video Chain.

The amplitude distribution of this noise is approximately Gaussian and has an upper frequency distribution approximately equal to the upper limit of the video-chain frequency response. Assuming a constant spectral distribution versus amplitude, the ratio of the signal threshold voltage to the RMS noise level for a fixed FAR is always a constant. Therefore, if this fixed constant and the RMS noise level were known, we would know at what level to set the signal threshold voltage for a constant FAR.

Figure 9 is the frequency spectrum of the post-detection noise. The 3-dB cutoff frequency, f_H, of the spectrum is approximately equal to the video bandwidth of the detector

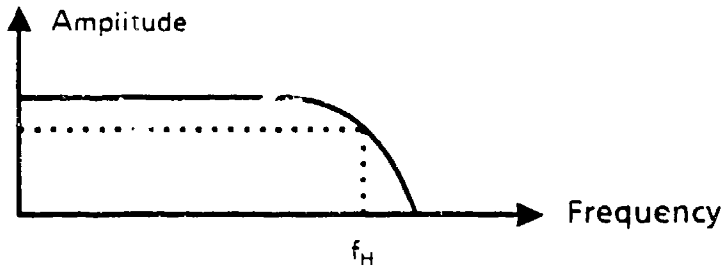

FIGURE 9. Frequency Spectrum of Post-Detection Noise.

linear-amplifier chain. For a single-pole rolloff this quantity can be measured by feeding a pulsed RF input to the detector and measuring the rise time at the video output. (This procedure assumes that the RF input pulse rise time is much greater than the video bandwidth.) The video bandwidth is then $BW_V = 0.35/t_r$, where t_r is the 10 to 90% rise time of the video output. Appendix A describes two methods of determining the video bandwidth of a detector-video-amplifier chain.

The amplitude distribution is normally the most important parameter to be considered, since we are interested in the peaks of the noise as a function of the RMS level of the noise. Figure 10 shows the amplitude probability-density function of post-detection noise, assuming a normal or Gaussian distribution. The amplitude density function is Gaussian with positive and negative amplitudes equally probable when $a = 0$ (equivalent to AC-coupled noise). We will find that detected receiver noise can have very different properties than post-detection noise.

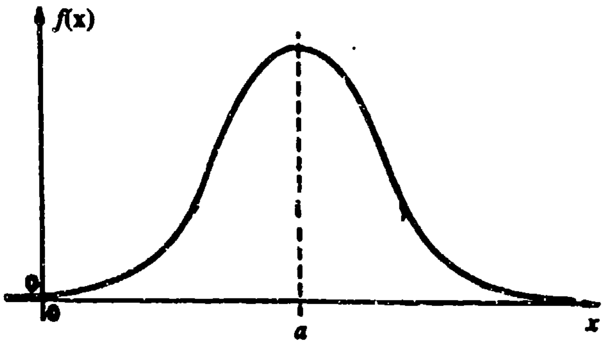

FIGURE 10. Density Function for Post-Detection Noise.

TEST DATA FOR POST-DETECTION NOISE

If we were to plot FAR_N, the normalized FAR, as a function of sigma ratio, where FAR_N and the sigma ratio are given by

$$FAR_N = FAR/FAR_{MAX}$$

$$\text{Sigma ratio} = V_{SIGTHR}/V_{RMS}$$

where FAR_{MAX} is the maximum FAR measured, we would find that the curve is also Gaussian-shaped if the noise is Gaussian in nature. FAR_{MAX} occurs at about $V_{SIGTHR} = 0$ volts when the noise is AC-coupled into the comparator. The maximum FAR is a complex function of the spectral content of the noise itself and the frequency limitations of the comparator and test equipment used to measure the FAR. V_{RMS} is the true RMS noise level.

Figure 11 shows the FAR distribution measurement test setup and Figures 12 through 19 show the actual test data for several cases of noise bandwidth using a low-frequency noise source followed with an adjustable single-pole, low-pass filter. The top figure for each case shows the spectral content of the noise at the comparator input while the bottom figure for each case shows the normalized FAR distribution versus the sigma ratio. The normalized

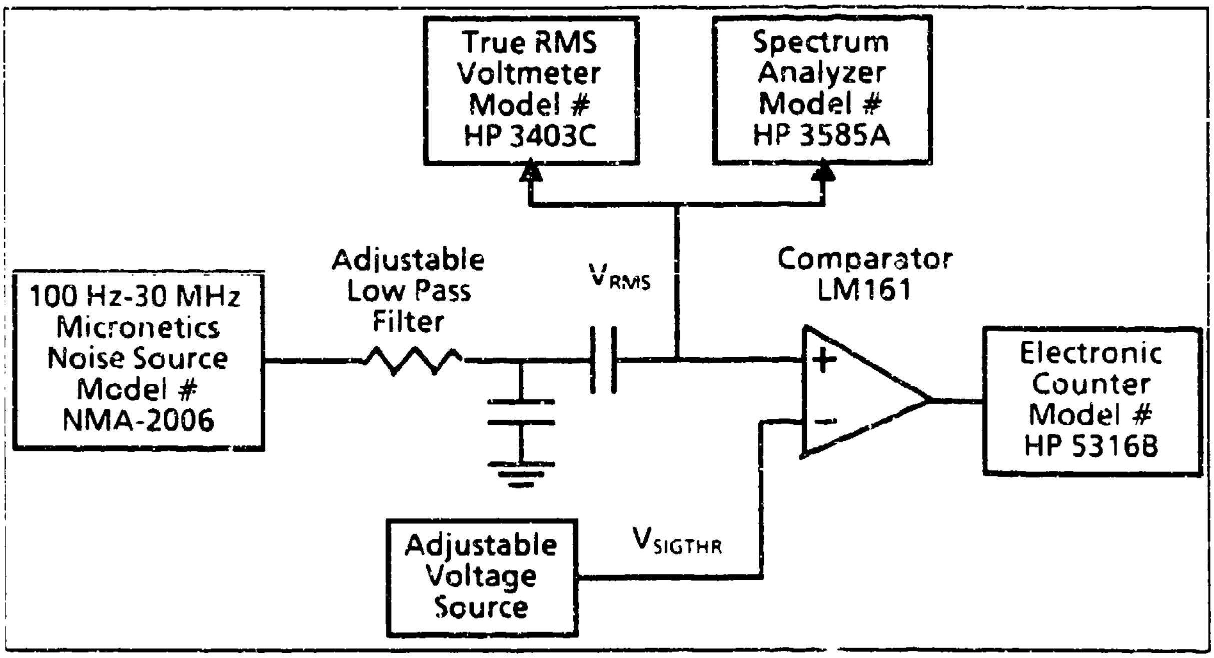

FIGURE 11. FAR Distribution Measurement Test Setup.

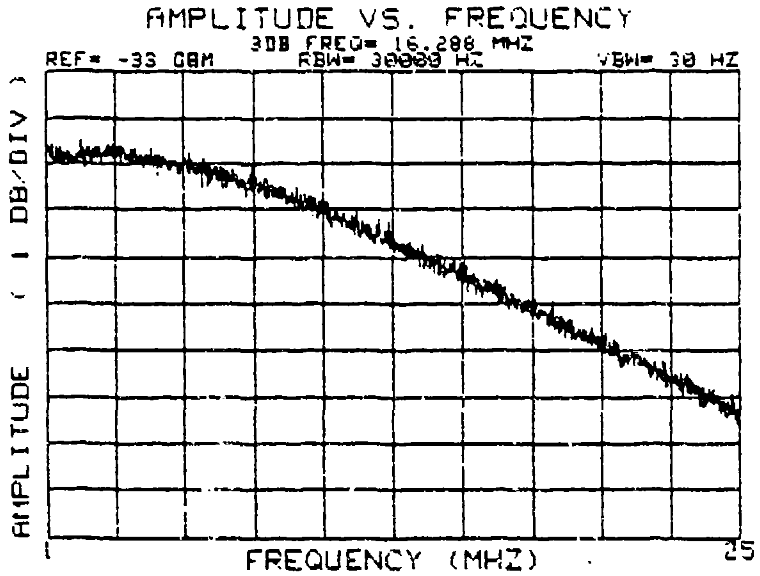

FIGURE 12. Spectral Distribution for Gaussian Noise Source; 3 dB Noise Bandwidth = 16.3 MHz.

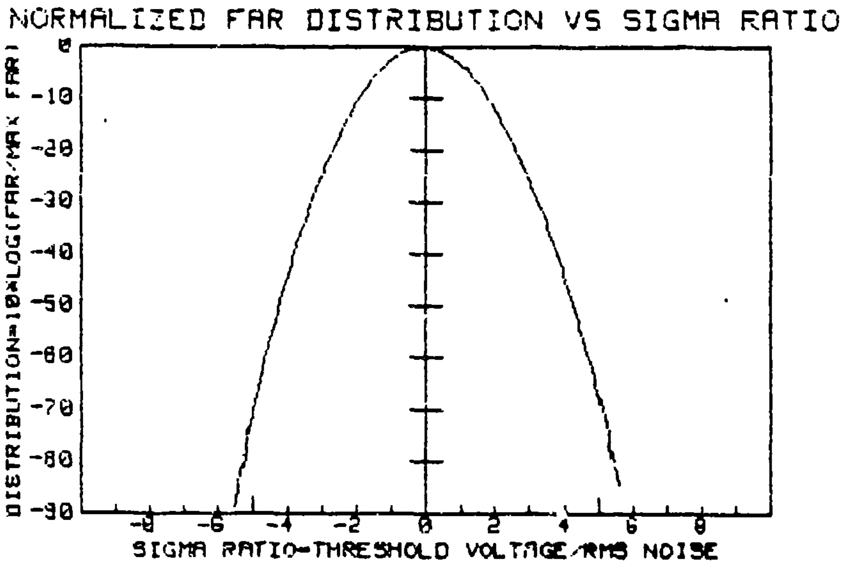

FIGURE 13. FAR Distribution for Gaussian Noise Source; FAR_{MAX} = 9.9 MHz.

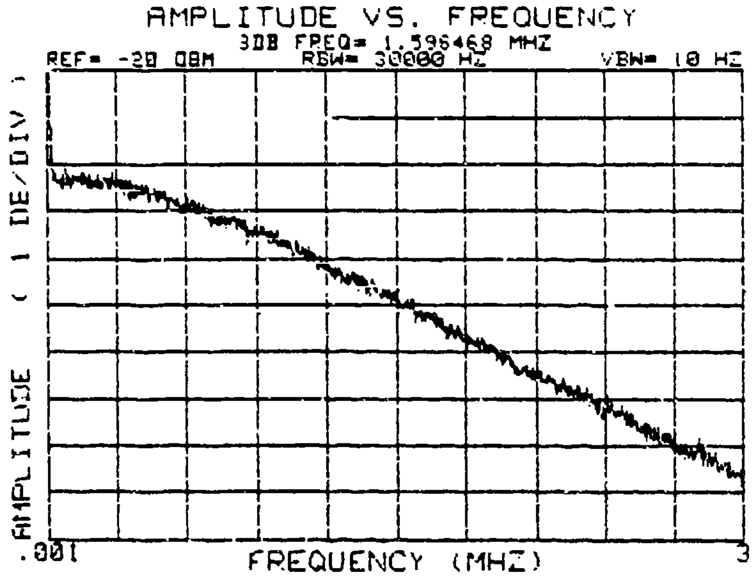

FIGURE 14. Spectral Distribution for Gaussian Noise Source: 3 dB Noise Bandwidth = 1.59 MHz.

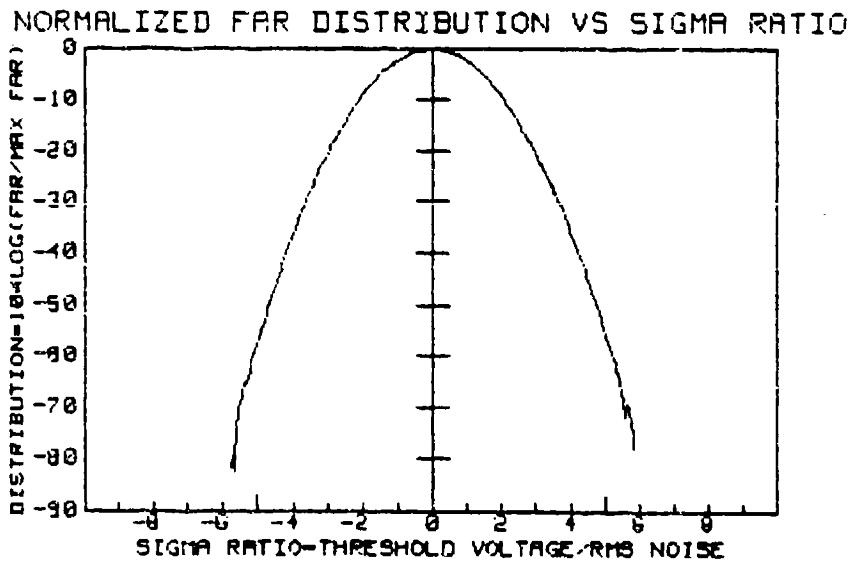

FIGURE 15. FAR Distribution for Gaussian Noise Source; FAR_{MAX} = 3.04 MHz.

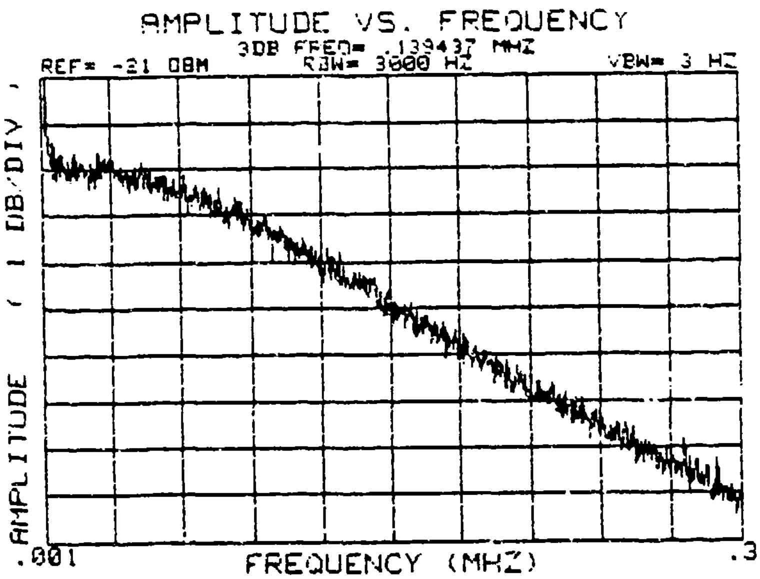

FIGURE 16. Spectral Distribution for Gaussian Noise Source; 3 dB Noise Bandwidth = 139 kHz.

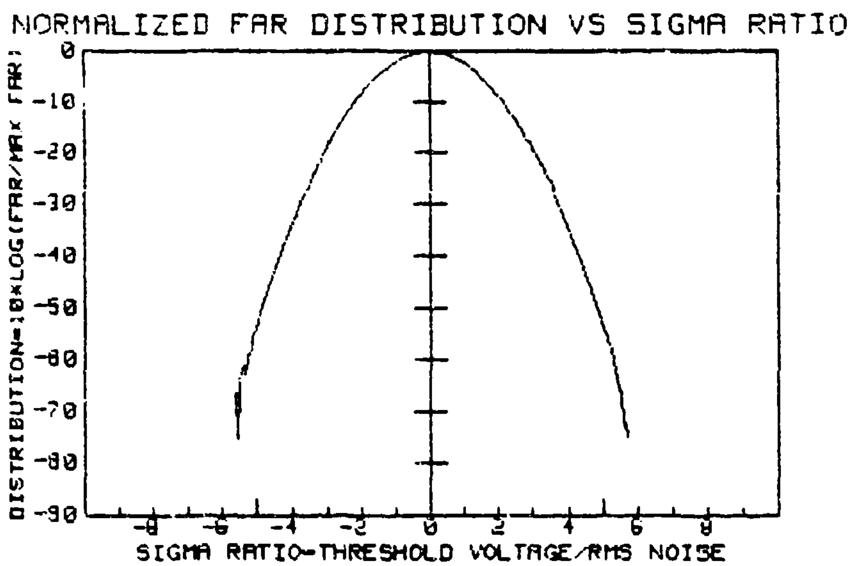

FIGURE 17. FAR Distribution for Gaussian Noise Source; FAR_{MAX} = 856 kHz.

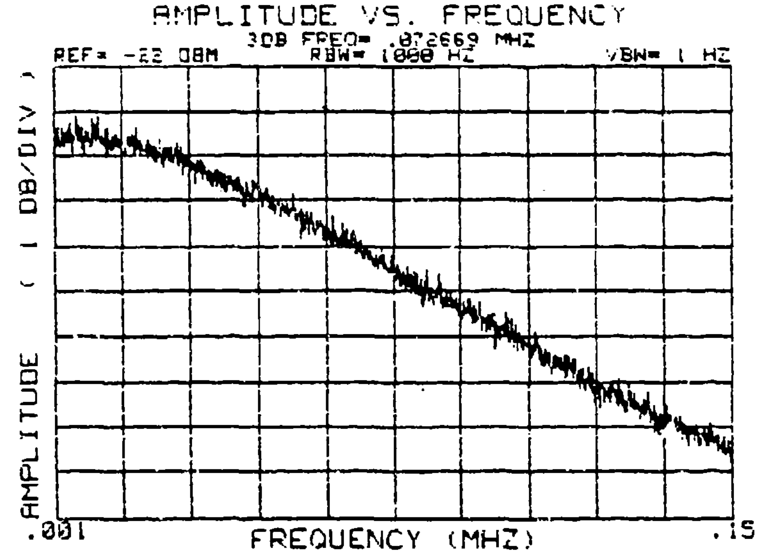

FIGURE 18. Spectral Distribution for Gaussian Noise Source; 3 dB Noise Bandwidth = 72.7 kHz

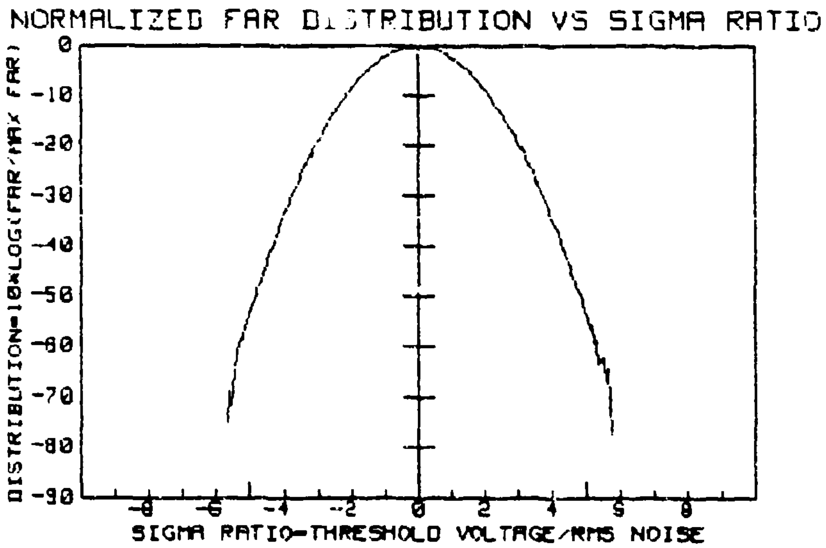

FIGURE 19. FAR Distribution for Gaussian Noise Source; FAR_{MAX} = 747 kHz

FAR distribution, FAR_N, is plotted on a logarithmic scale because of the very wide dynamic range of FARs measured. Figure 20 shows the detector video amplifier chain designed by Richard S. Hughes of NWC to replace the Micronetics noise source and low-pass filter of Figure 11. The spectral and FAR distribution for the output of the NWC-designed detector video-amplifier chain (with linear post-amplification) is given in Figures 21 and 22. Note that the detector video amplifier normalized FAR distribution follows the same normalized FAR distribution as the Gaussian noise source. The most important aspect of the FAR distribution plots is the common shape of the curve regardless of the noise bandwidth.

DETECTED NOISE CHARACTERISTICS WITH LINEAR POST-AMPLIFICATION

Figure 23 shows a detector stage preceded by RF amplification with an RF bandwidth-limiting filter and linear post-detection amplification. The detected noise present at the video output is due to the internal broadband noise of the RF amplifier and preceding components (i.e. mixers, LOs, etc.) mixing with itself in the detector (Reference 1). For relatively low RF gains, this noise is negligible with respect to the post-detection noise.

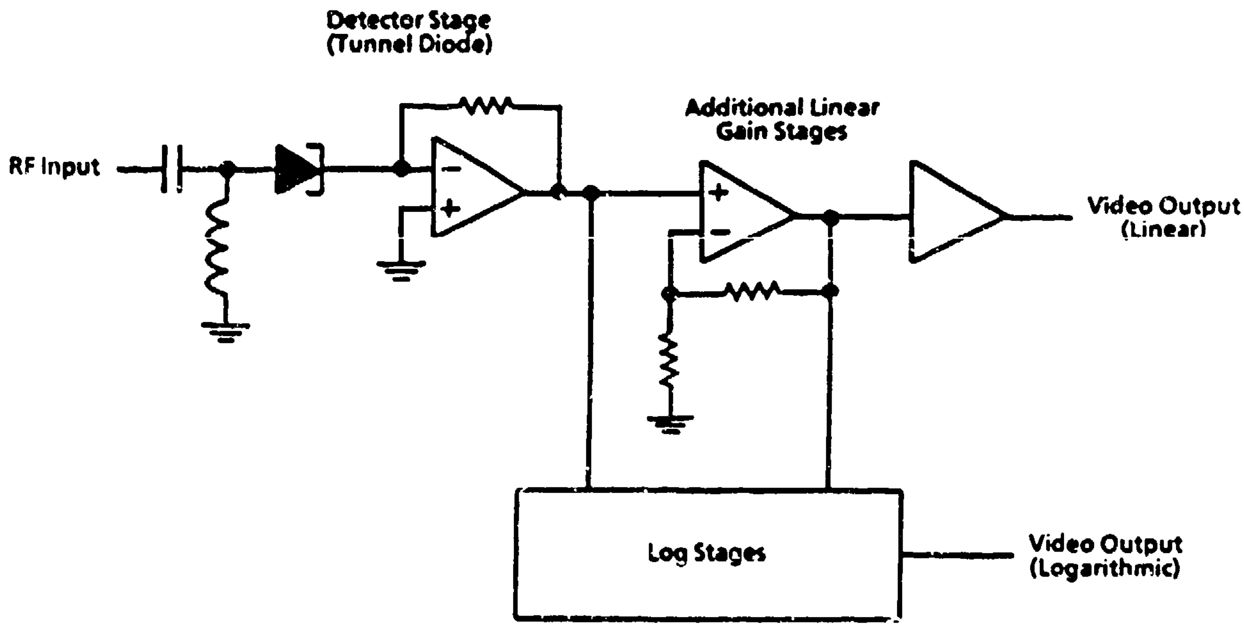

FIGURE 20. Detector Video Amplifier Chain.

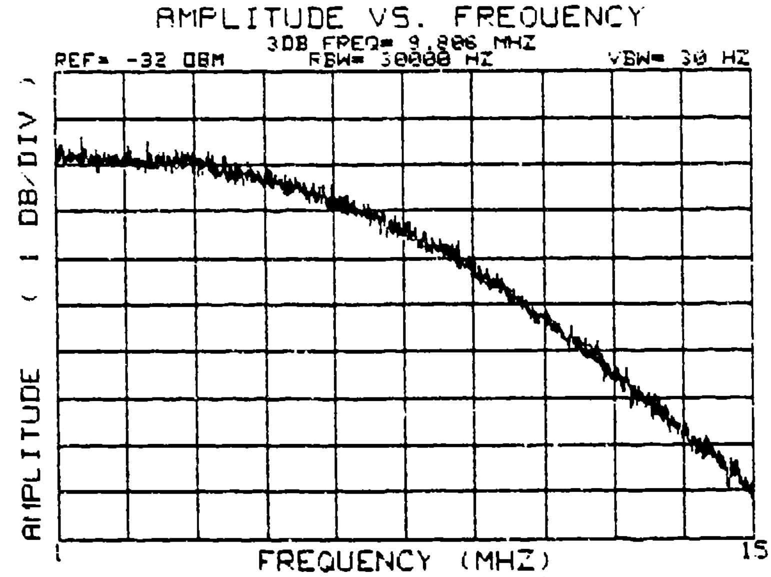

FIGURE 21. Spectral Distribution for Post-Detection Noise (Linear Output); 3 dB Noise Bandwidth = 9.81 MHz.

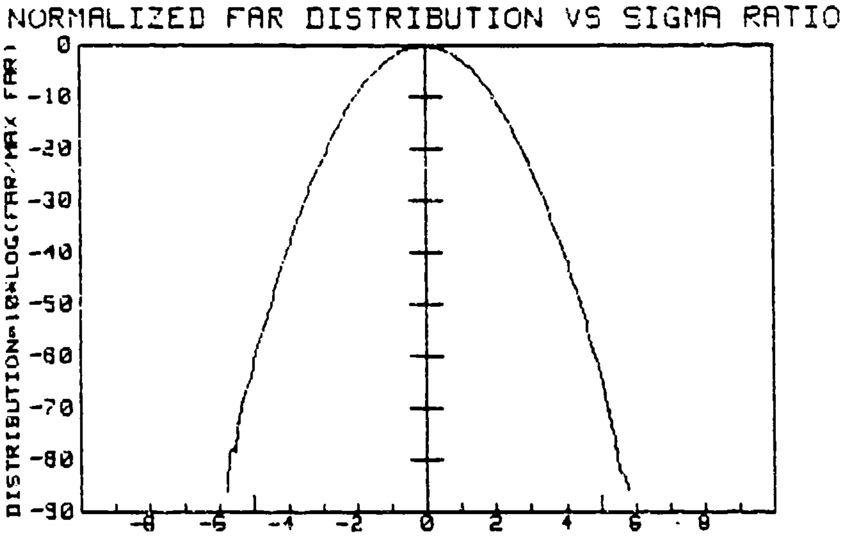

FIGURE 22. FAR Distribution for Post-Detection Noise (Linear Output); FAR_{MAX} = 6.62 MHz.

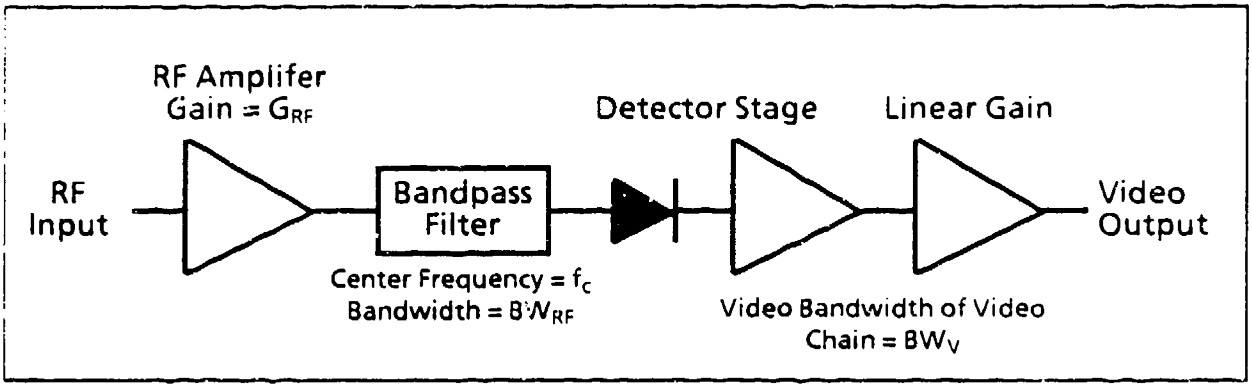

FIGURE 23. Envelope Detector System With RF Preamplification.

Figure 24 shows the center frequency of the frequency spectrum of the noise at the input and output of the detector. Assume that the bandpass filter is much greater than the bandwidth of the bandpass filter. For any given BW_{RF}, the detector output will have a noise spectrum of $\frac{1}{2}BW_{RF}$*.

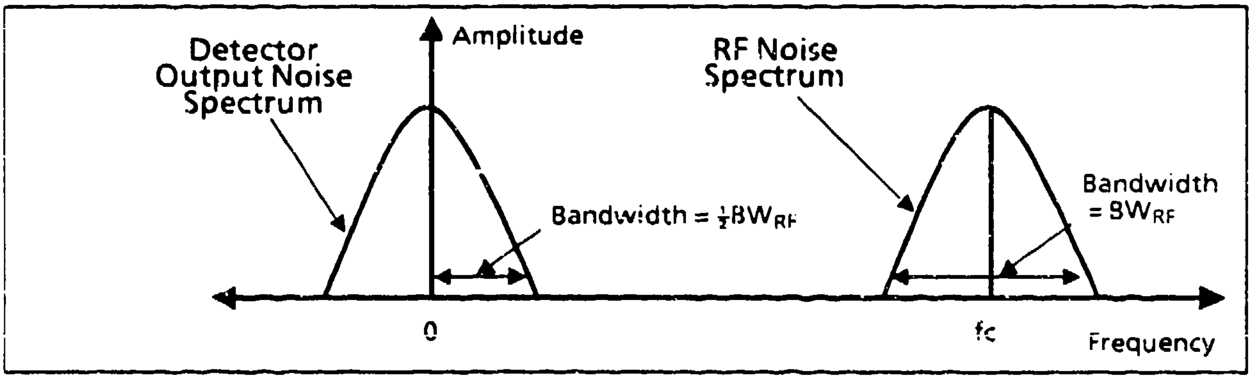

FIGURE 24. Frequency Spectrum of RF and Detected RF Noise.

The detected noise characteristics at the video output are dependent on BW_{RF}, the characteristics of the detector (i.e., linear or square-law), and the bandwidth of the detector and video stage.

* For simplicity, we will equate the RF noise bandwidth to the 3-dB bandwidth. Many authors refer to an equivalent noise bandwidth. See Reference 2 for a discussion of equivalent noise bandwidth.

The most important factor determining the noise characteristics at the video output is the ratio of the RF bandwidth to the video bandwidth. Throughout this report, we will refer to this ratio as the RF-to-video bandwidth ratio. In equation form this becomes

$$\text{RF-to-video bandwidth ratio} = (BW_{RF}/BW_V)$$

For optimum sensitivity, this ratio is chosen to be equal to 2.0 to meet matched filter criteria. However, for various reasons, this is seldom the case. For example, many EW systems have a wide RF bandwidth for large frequency coverage, so that they have a higher probability of acquiring a target of an unknown frequency. On the other hand, systems may need a narrow RF bandwidth to filter out unwanted targets in a dense RF environment.

The reason that this ratio is so important can be seen by analyzing Figure 25, which shows the noise at the output of the bandpass filter. The noise can resemble a sine wave oscillating at a frequency of f_c, the center frequency of the bandpass filter. The sine wave's amplitude and phase vary at a rate determined by the bandpass filter's bandwidth. Schwartz* found that the envelope of this noise follows Rayleigh rather than Gaussian statistics. If the video bandwidth is great enough to pass all the components of this envelope, then the noise at the video output will also follow Rayleigh statistics. Similarly, the FAR distribution will also follow Rayleigh statistics.

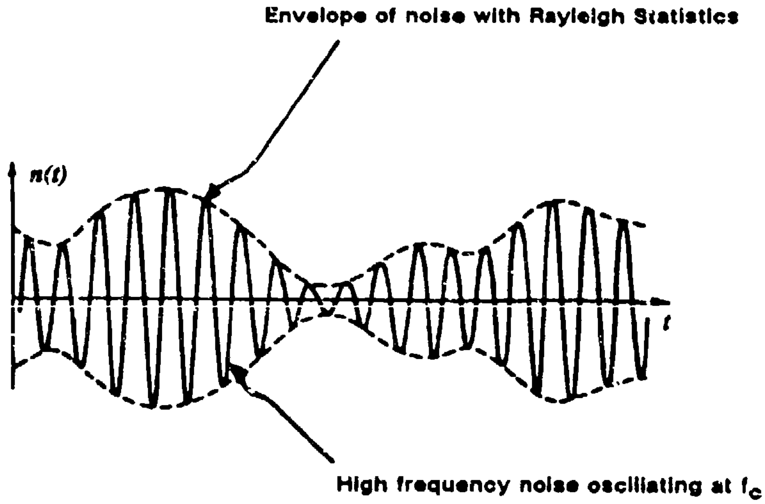

FIGURE 25. Noise at Output of Narrow-Band Filter. (Extracted from Reference 3).

* Schwartz (Reference 3, pp. 363-369) discusses a mathematical model for narrow-band noise from which the above discussion was taken.

Figure 26 shows the detector output-noise spectrum and two special cases of relative video bandwidth. The case of $BW_V \gg BW_{RF}$ will produce video noise that will be highly Rayleigh-distributed. The case of $BW_V \gg BW_{RF}$ will produce video noise that is Gaussian-distributed. It follows that the FAR distribution will also follow this same behavior. The next section contains test data for the FAR distribution of several cases of BW_{RF}/BW_V.

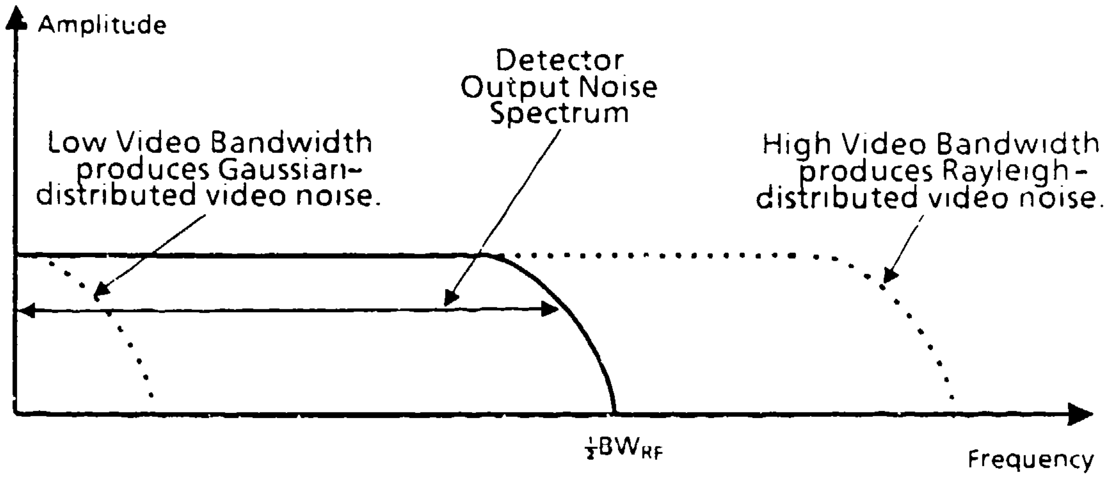

FIGURE 26. Spectrum of Detected RF Noise and Video Bandwidth.

TEST DATA FOR DETECTED NOISE

This section contains FAR distribution data for detected noise. Figure 27 shows the specialized case of feeding a broadband noise source that covers the entire video and RF spectrum directly into the detector. The noise produced for this case is still very Gaussian, indicating that the Rayleigh distribution is caused by the detector shifting the RF noise spectrum down to DC.

The FAR distribution data for several values of (BW_{RF}/BW_V) are given in this section. Figure 28 show the FAR distribution data for the case where $BW_{RF}/BW_V = 450$. Even for this ratio, the video output contains noise that is partially Rayleigh-distributed. As BW_{RF}/BW_V decreases (Figures 29 through 33), the FAR distribution becomes increasingly asymmetrical around the average value (0 volts) and follows a Rayleigh-type distribution. For all tests performed, the RF gain of the test receiver was set to a level such that the video output noise increased by a factor of at least 5. This setting was made to ensure that the video output noise was predominantly detected receiver noise.

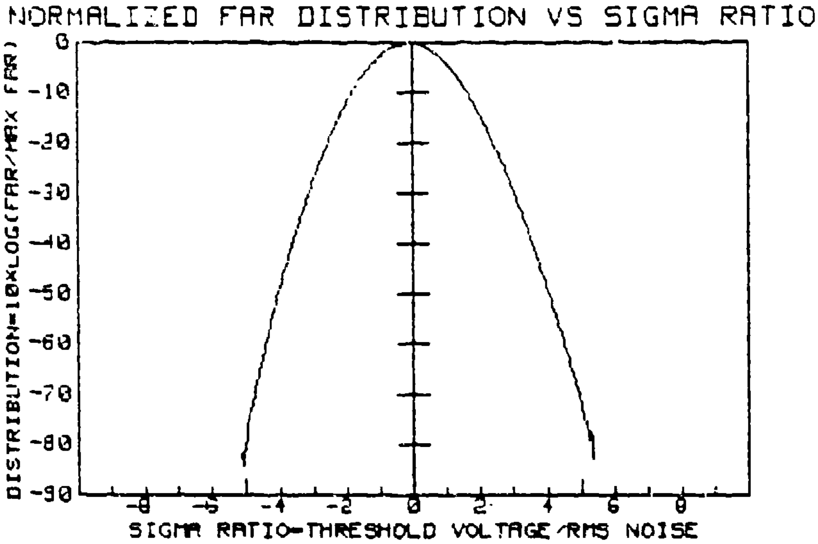

FIGURE 27. FAR Distribution for Broadband Noise Source Fed Directly Into the Detector.

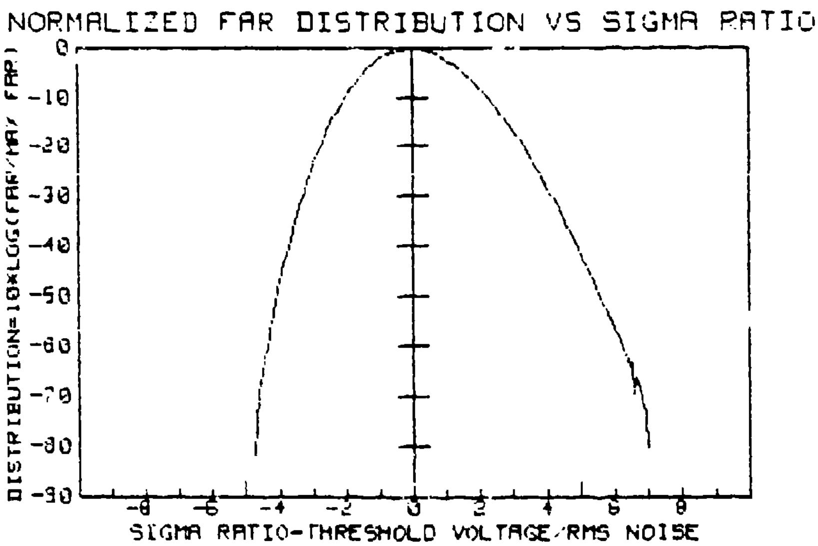

FIGURE 28. FAR Distribution for $BW_{RF}/BW_V = 450$.

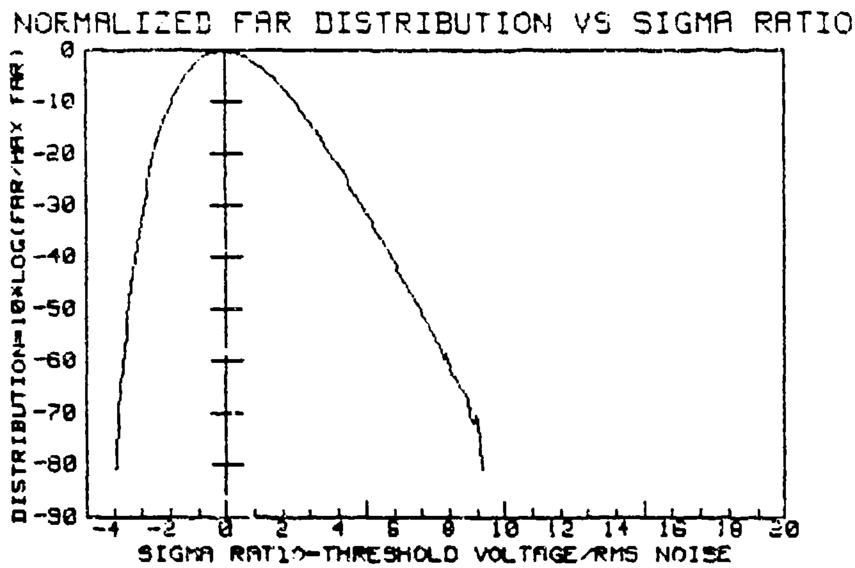

FIGURE 29. FAR Distribution for $BW_{RF}/BW_V = 75$.

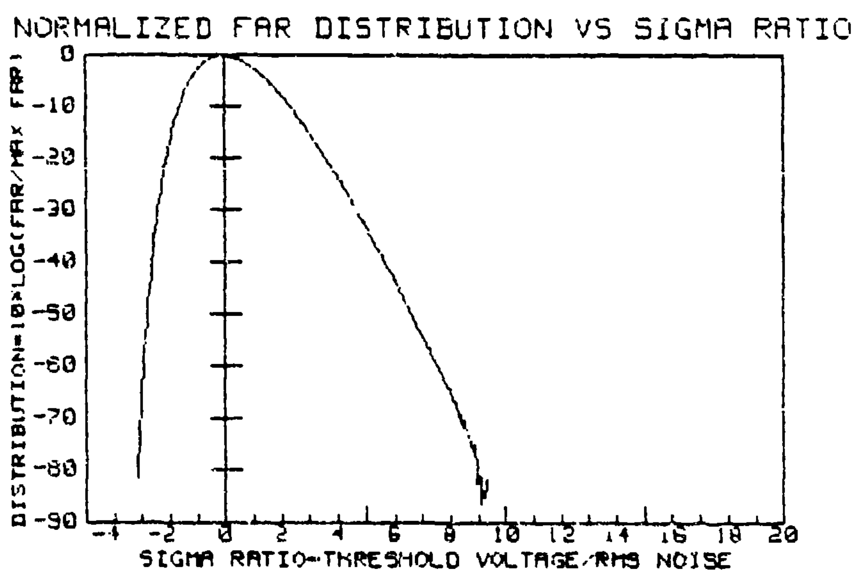

FIGURE 30. FAR Distribution for $BW_{RF}/BW_V = 25$.

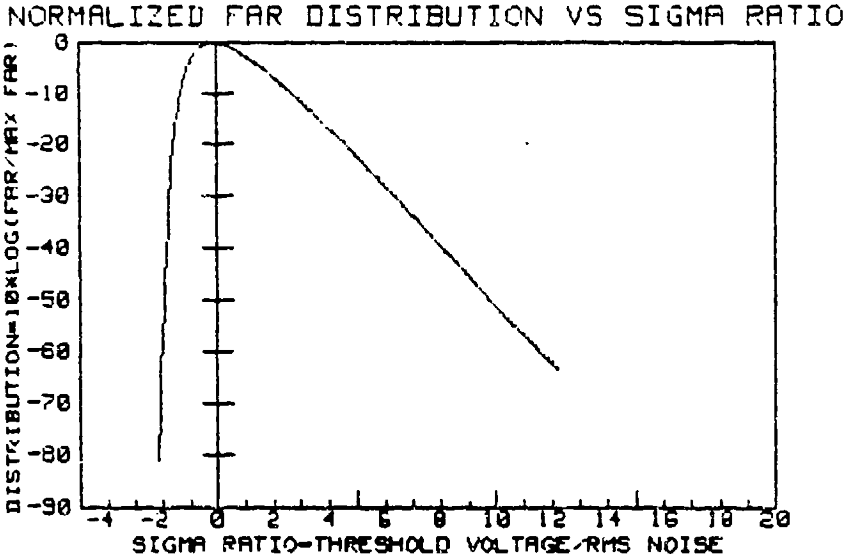

FIGURE 31. FAR Distribution for BW_{RF}/BW_V = 4.

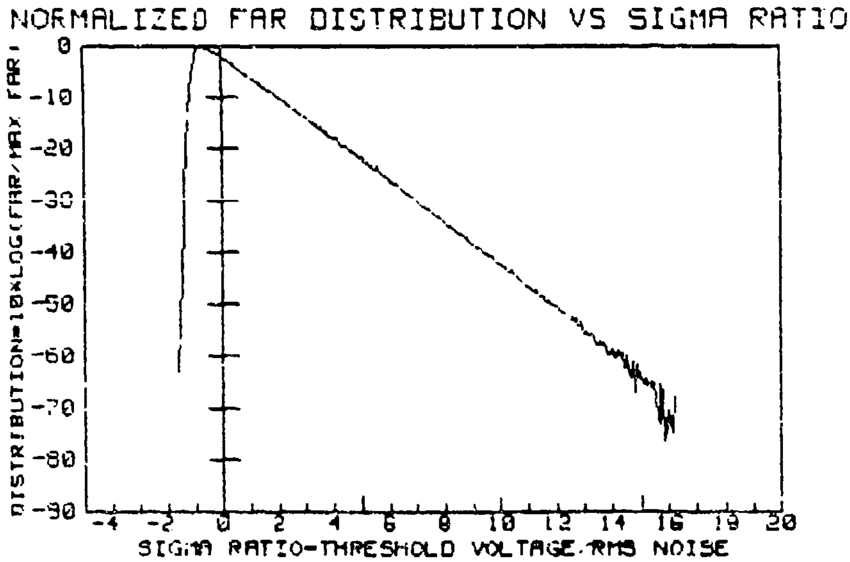

FIGURE 32. FAR Distribution for BW_{RF}/BW_V = 0.6.

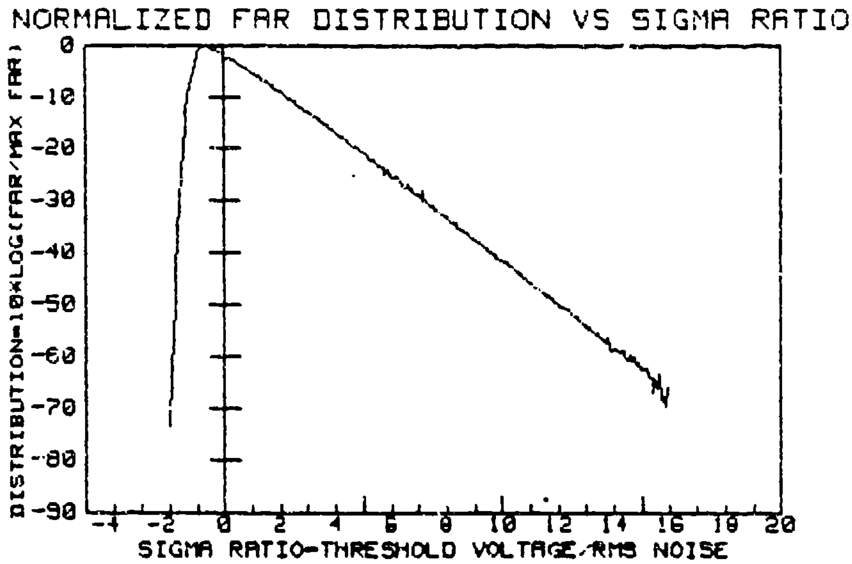

FIGURE 33. FAR Distribution for $BW_{RF}/BW_V = 0.03$.

Figures 32 and 33 show that for $BW_{RF}/BW_V < 1$, the video output noise is highly Rayleigh-distributed. Observe the linear portion of the FAR distribution for noise that is heavily Rayleigh-distributed. Since the FAR is plotted on a logarithmic scale, this plot indicates the raw FAR to be exponentially distributed. Rayleigh distribution is sometimes referred to as exponential distribution.

LINEAR POST-AMPLIFICATION SUMMARY

The previous sections have attempted to describe the noise characteristics at the video output of a square-law envelope-detector system preceded by RF amplification. Post-detection noise is Gaussian in nature and has it origins in the detector and video amplifiers. Post-detection noise is the type of noise that occurs with no RF preamplification present. When sufficient RF preamplification is present, receiver noise from the RF electronics contributes noise at the video output. Depending upon the video and RF bandwidths, this detected noise can vary from Gaussian to Rayleigh in nature. Appendix B gives a simple technique that used an oscilloscope to determine the extent of Rayleigh distribution at the video output of an envelope detector system.

In summary, the amount of "Rayleighness" of the noise at the video output contributed by the receiver is a strong function of the ratio of the RF bandwidth to the video bandwidth.

The smaller this ratio. the more Rayleigh-distributed is the noise at the video output. Table 1 shows the positive and negative sigma ratios (V_{SIGTHR}/V_{RMS}) necessary to decrease the normalized FAR ratio (FAR/FAR_{MAX}) by a factor of 10^6. For Gaussian noise, this ratio is approximately equal to 5.2. For very low BW_{RF}/BW_V, this ratio increases to approximately 14.5.

TABLE 1. Sigma Ratios for Various Values of BW_{RF}/BW_V.

BW_{RF}/BW_V	Sigma ratios for $FAR/FAR_{MAX} = 10^{-6}$	
	Positive sigma ratio	Negative sigma ratio
Gaussian noise	5.2	-5.2
450	6.2	-4.4
75	8.0	-3.8
25	7.7	-3.0
4	11.4	-2.0
0.6	14.1	-1.7
0.03	14.5	-1.8

Of particular interest is how quickly the transition from Gaussian to Rayleigh takes place. The transition is almost fully complete before the true RMS level of the noise doubles. This characteristic makes the transition very hard to handle if a constant FAR is to be obtained over this transition region. Figures 34 through 37 show the normalized FAR

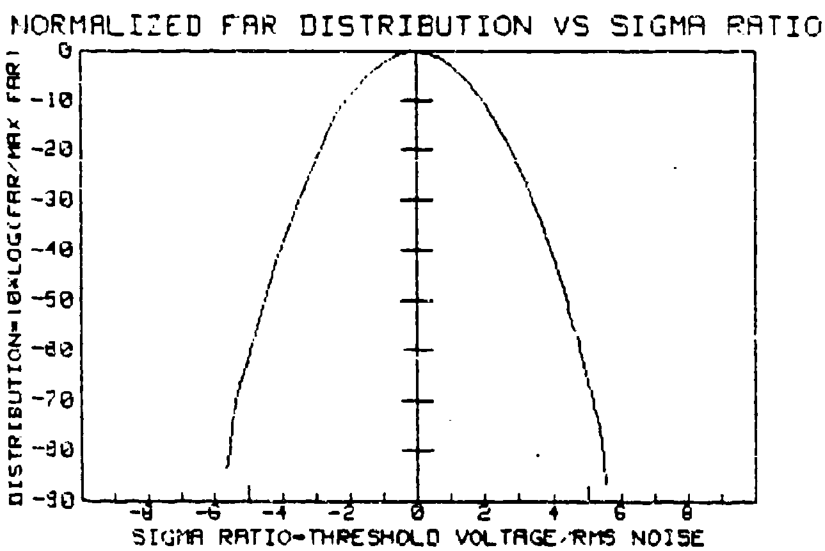

FIGURE 34. FAR Distribution With No RF Gain;
V_{RMS} = 27.8 mV.

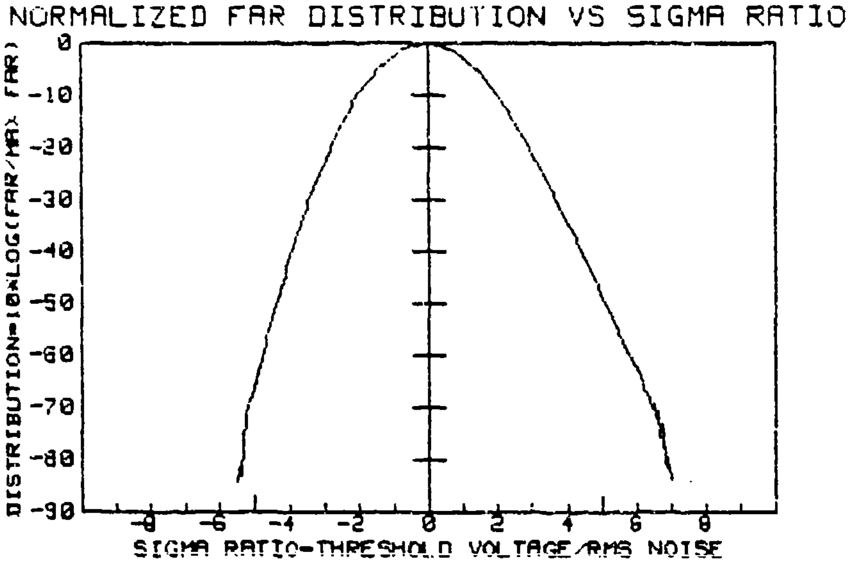

FIGURE 35. FAR Distribution for 44.5 dB RF Gain; V_{RMS} = 29.5 mV.

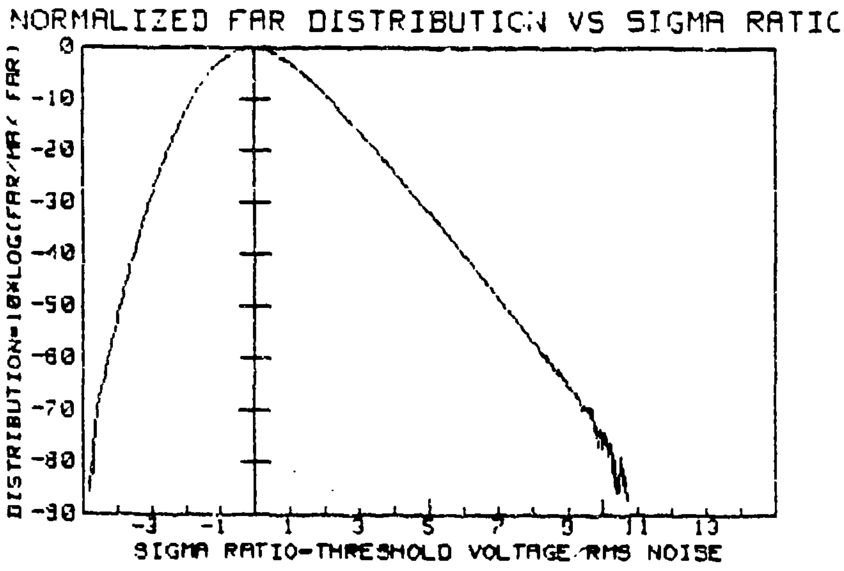

FIGURE 36. FAR Distribution for 49.5 dB RF Gain; V_{RMS} = 35.8 mV.

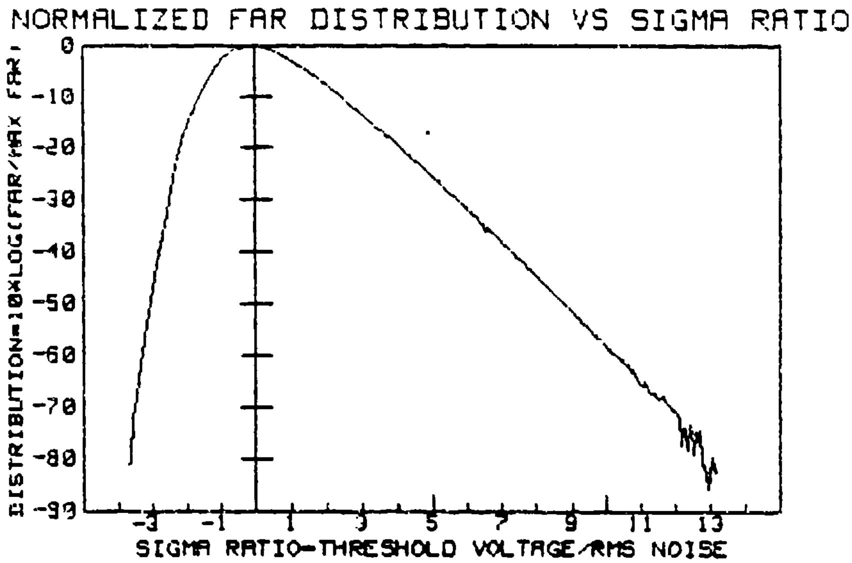

FIGURE 37. FAR Distribution for 53.5 dB RF Gain; V_{RMS} = 54.5 mV.

distribution for BW_{RF}/BW_V = 4 for various RF gains and corresponding RMS noise levels as the linear output transitions from Gaussian to Rayleigh distribution.

Referring once again to the adaptive signal threshold proposed in the introduction and shown earlier in Figure 7, suppose we wanted to maintain a FAR of about 10 Hz. What value of K is needed to maintain this FAR at the linear output of an envelope detector system?

Table 2 shows the test data (BW_V = 10.0 MHz and BW_{RF} = 40 MHz) for the positive sigma ratios necessary to maintain a FAR of approximately 10 Hz as a function of the video output RMS-noise level. The value is constant for the case of post-detection noise only. The value is also constant when the detected noise starts to dominate.

NOISE CHARACTERISTICS WITH LOGARITHMIC POST-AMPLIFICATION

Figure 38 shows the envelope detector system discussed previously except with logarithmic instead of linear post-amplification. This figure shows a typical EW system in which the logarithmic amplifier compresses the wide dynamic range of signals from the detector. Usually, the logarithmic amplifier is a piecewise approximation of a true logarithmic transfer function (Reference 4).

TABLE 2. Positive Sigma Ratios of FAR = 10 Hz for Various RMS Noise Levels (Linear Output).

RMS noise level, mV	Value of K for FAR = 10 Hz.
27.2	4.73
28.5	4.88
29.5	5.65
32.3	6.91
35.8	8.12
42.3	8.76
54.5	9.82
63.1	10.21
70-200	10.7-11

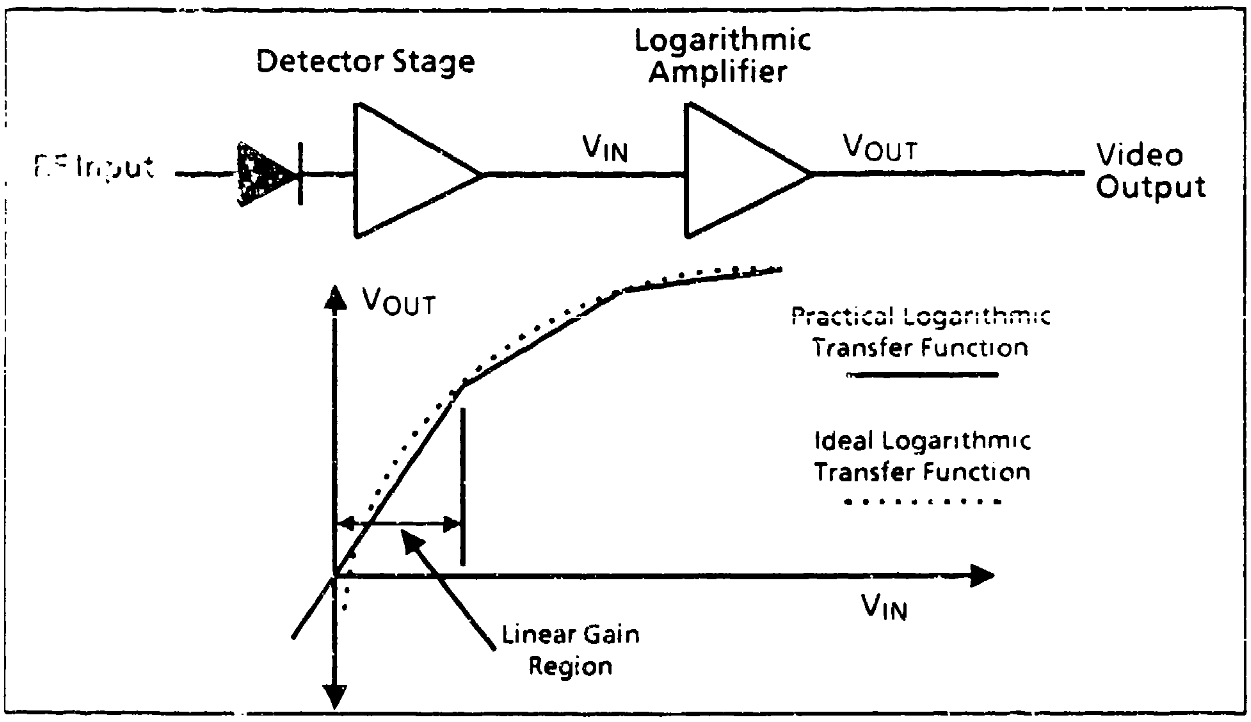

FIGURE 38. Envelope Detector With Logarithmic Post Amplification.

Although the logarithmic transfer function is invaluable for compressing the dynamic range of the detector output, it further complicates the nature of the noise at the video output. Not only is the amplitude distribution of the noise at the video output dependent on the relative amounts of post-detection and detected noise, but also upon the magnitude of the noise entering the logarithmic amplifier. Since the gain for a high-level signal is less than that of a low-level signal, we can expect the peaks of the noise to be compressed more than the RMS level of the noise. Therefore, the crest factor (peak-to-RMS ratio) will decrease with increasing signal level.

Note the region of linear gain in the lower portion of the practical logarithmic transfer function of Figure 38. For low noise or signal levels, the logarithmic amplifier will behave as if it were a linear amplifier. Therefore, the noise characteristics for noise levels in this region will be the same as those discussed in the previous section for the case of linear post-amplification.

As the noise at the input of the logarithmic amplifier increases, the peaks of the noise become compressed at a much greater rate than the effective RMS level of the noise.

In summary, four possible types of amplitude and FAR distributions can be present at the output of a detector logarithmic amplifier preceded by RF amplication. These four distributions are

1. **Gaussian.** If the linear-logarithmic transition input of the logarithmic amplifier has not been reached and detected noise is not present, then the amplitude and FAR characteristics will be Gaussian-distributed.

2. **Compressed Gaussian.** If the linear-logarithmic transition input of the logarithmic amplifier has been reached and no detected noise is present, then the amplitude and FAR distribution will be what can be termed a "compressed" Gaussian distribution. The actual distribution will be dependent on the compression characteristics of the logarithmic amplifier.

3. **Rayleigh.** If detected noise is present and the linear-logarithmic transition input has not been reached, then the amplitude and FAR distribution will be Rayleigh-distributed. The actual distribution will be dependent upon the RF-to-video bandwidth ratio as discussed in the previous section.

4. **Compressed Rayleigh.** If detected noise is present and the linear-logarithmic transition input has been reached, then amplitude and FAR distribution will be a "compressed" Rayleigh distribution. The actual distribution will be dependent on the compression characteristics of the logarithmic amplifier and also the RF-to-video bandwidth ratio.

The next section contains actual test data for the FAR distribution of a logarithmic amplifier output.

TEST DATA FOR LOGARITHMIC POST-AMPLIFICATION

This section contains actual test data for the FAR distribution at the output of a logarithmic amplifier. The RF-to-video bandwidth ratio for all tests was approximately equal to 4.

The first test was the FAR distribution with no receiver noise entering the detector. For this type of logarithmic amplifier, the FAR distribution is still primarily Gaussian. Subsequent data points were taken by increasing the amount of receiver noise entering the detector (this was done by increasing the amount of receiver gain and measuring the FAR distribution). In this manner, it was easy to see the FAR distribution transition from Gaussian to Rayleigh and then to a compressed Rayleigh distribution. The output voltage at which compression for the logarithmic amplifier tested starts is approximately 200 mV.

Figure 39 is the FAR distribution for the case of no receiver noise entering the detector. Compare this curve to the Gaussian-noise source curves (Figures 13, 15, 17, and 19). Figures 40 through 43 are test data for increasing amounts of receiver noise.

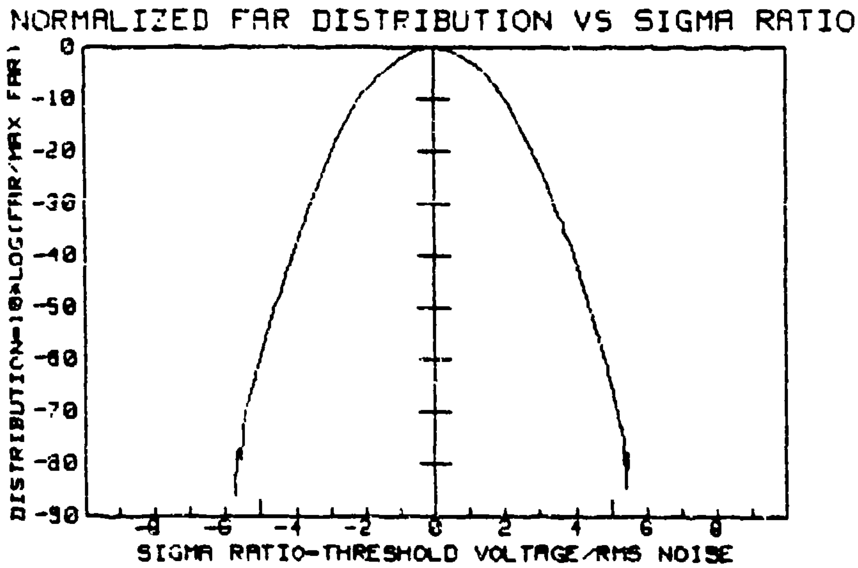

FIGURE 39. FAR Distribution for Logarithmic Amplifier Output; V_{RMS} = 33 mV.

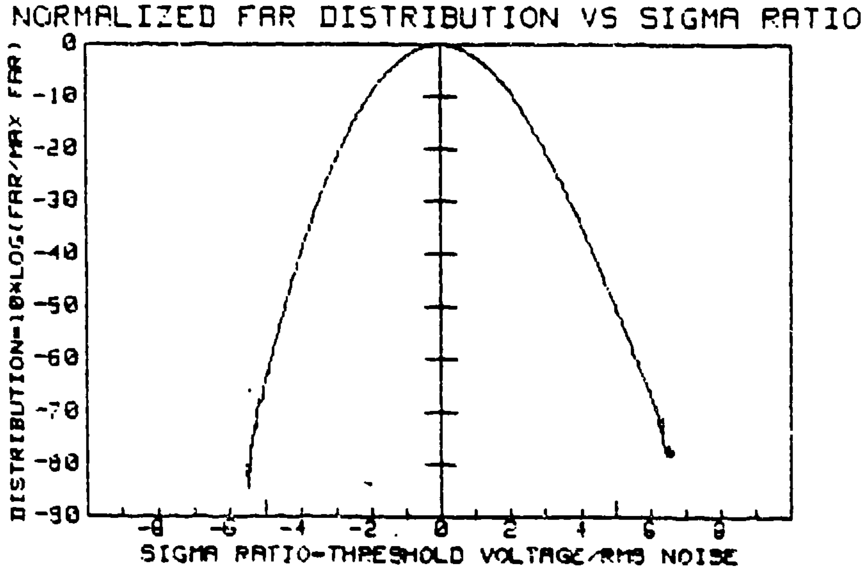

FIGURE 40. FAR Distribution for Logarithmic Amplifier Output; V_{RMS} = 38 mV.

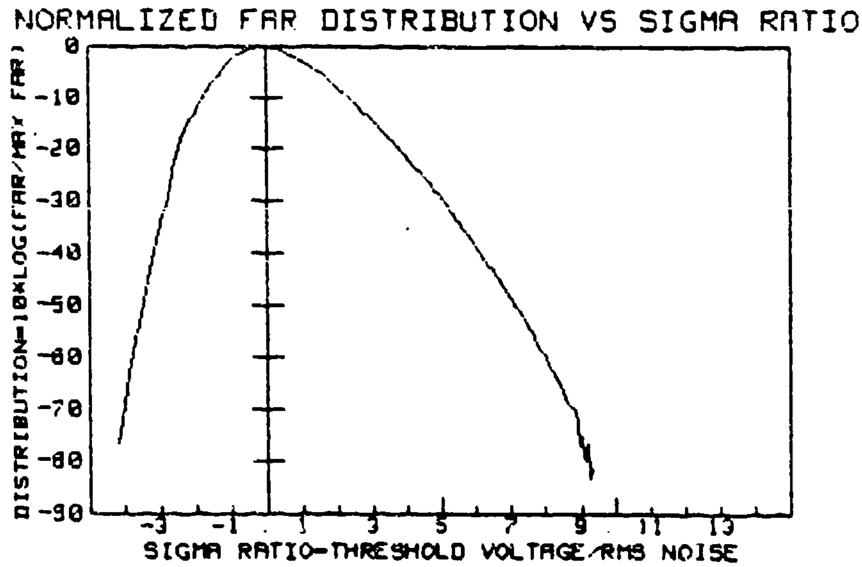

FIGURE 41. FAR Distribution for Logarithmic Amplifier Output; V_{RMS} = 58 mV.

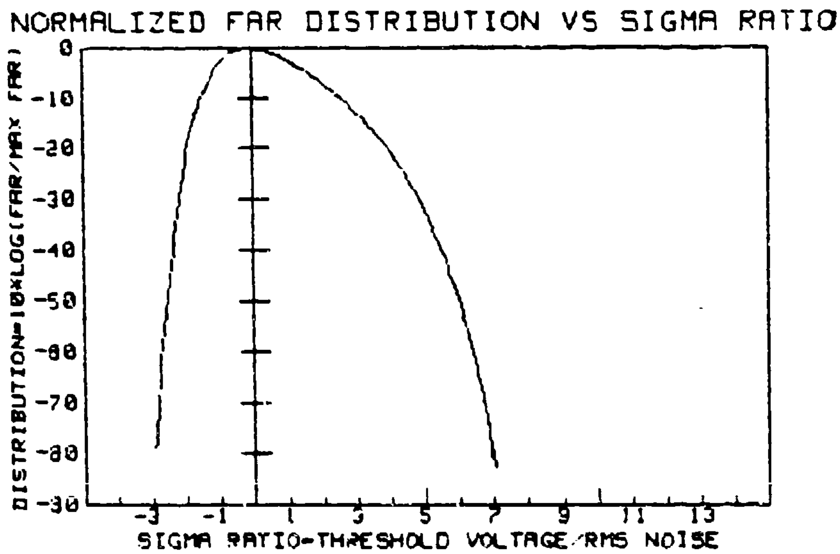

FIGURE 42. FAR Distribution for Logarithmic Amplifier Output; V_{RMS} = 114 mV.

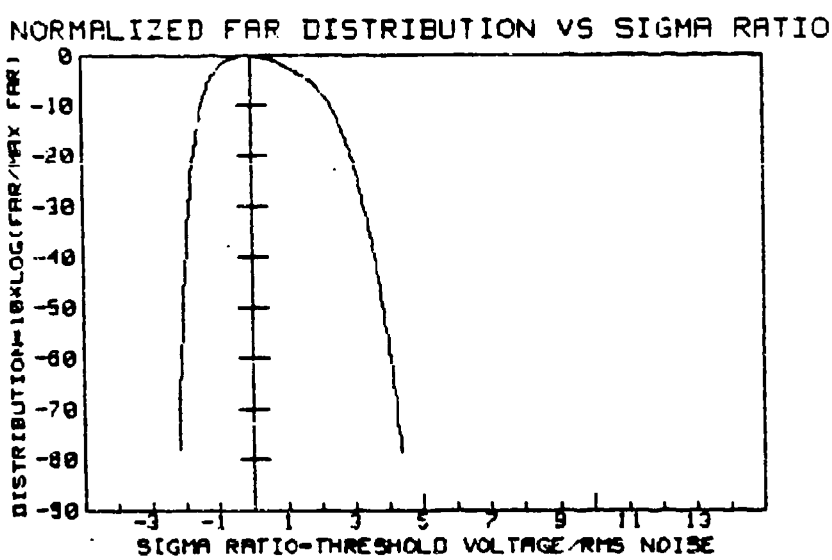

FIGURE 43. FAR Distribution for Logarithmic Amplifier Output; V_{RMS} = 256 mV.

LOGARITHMIC POST-AMPLIFICATION SUMMARY

The previous sections have attempted to describe the noise characteristics at the video output of the logarithmic amplifier. It has been shown that the amplitude and FAR distribution of the noise can vary from Gaussian to Rayleigh to a compressed distribution of each. In summary, the actual distribution will be dependent on the following parameters:

1. The relative amounts of detected and post-detection noise.

2. The RF-to-video bandwidth ratio.

3. The compression characteristics of the logarithmic amplifier.

4. The amplitude of the noise entering the logarithmic amplifier (this is actually implied under parameter no. 3).

Referring again to the adaptive signal threshold proposed in the introduction and in the linear post-amplification summary (see figure 7), suppose we wanted to maintain a FAR of 10 Hz with logarithmic post-amplification. What is the value of K needed to maintain this FAR at the logarithmic output of an envelope detector system?

Table 3 shows actual test data of the positive sigma ratios necessary to maintain a FAR of approximately 10 Hz as a function of the video-output RMS-noise level. It is interesting to note that the compression for high noise levels is so great that the 10-Hz sigma ratio becomes less than the 10-Hz sigma ratio for Gaussian-distributed noise.

TABLE 3. Positive Sigma Ratios of FAR = 10 Hz for Various RMS Noise Levels (Logarithmic Output).

RMS noise level, mV	Value of K for FAR = 10 Hz
36	4.70
38	5.45
58	7.73
69	7.65
81	7.26
114	6.26
170	4.96
256	4.00

Appendix A

DETERMINING VIDEO BANDWIDTH

Measuring the video bandwidth of the detector video-amplifier chain is not as simple as one might think. Usually, the simplest method is to input a very fast rise time RF pulse (much faster than the anticipated video bandwidth) and then measure the rise time at the video output. The video bandwidth is then given by

$$BW_V = 0.35/t_r$$

where t_r is the video output rise time (Reference 5).

Although this is a quick and simple method, it has several limitations: (1) slew rate limitations may give inaccurate results; (2) it is only accurate for a single-pole rolloff slope; (3) the constant coefficient, 0.35, changes if the post-amplification is logarithmic; and (4) this method does not show the actual noise-spectrum amplitude as a function of frequency.

Another method can be used if the center frequency and the low cutoff frequency of the bandpass filter are both much greater than the anticipated video bandwidth. The method is illustrated in Figure A-1.

A broadband noise source that is flat across the frequency range of the bandpass filter is first band-limited by the bandpass filter and then fed into the detector input. Assuming the broadband noise source produces noise at the video output that is much greater than the post-detection noise level, the noise spectrum at the video output is essentially the frequency rolloff of the detector video-amplifier chain. A practical example is given below.

Consider an envelope detector system with the following parameters:

f_c = 1.0 GHz
BW_{RF} = 500 MHz
Broadband noise frequency range = 500 to 1500 MHz

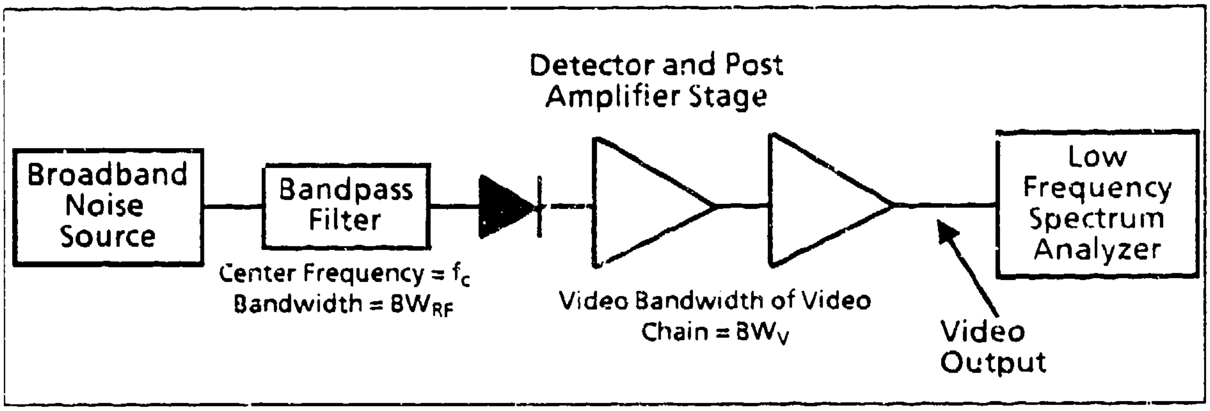

FIGURE A-1. Block Diagram of Video-Bandwidth Measurement Method.

The anticipated bandwidth of the detector video-amplifier chain is approximately 10 MHz. To measure the video bandwidth accurately, the detector output-noise spectrum should be fairly flat and also be much greater than the anticipated video bandwidth.

Figure A-2 shows the detected noise spectrum and the approximate video bandwidth. Note that the detector output-noise spectrum extends to approximately $\frac{1}{2} BW_{RF}$. Since the detected noise spectrum is essentially flat out to frequencies much greater than the video bandwidth, the noise spectrum at the video output is essentially a plot of the rolloff characteristics of the detector video-amplifier chain

Figure A-3 shows an actual spectrum analyzer plot of the output of a detector video-amplifier chain.

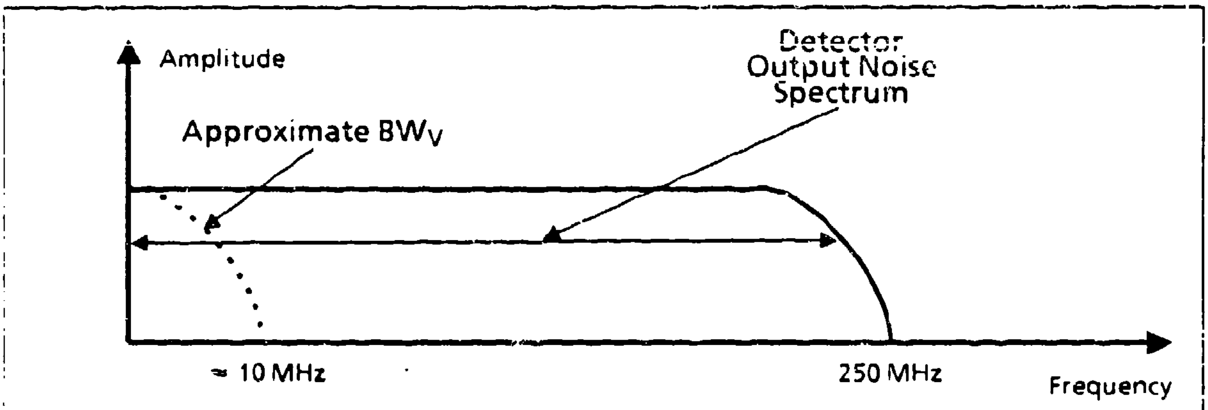

FIGURE A-2. Spectrum of Detected RF Noise and Video Bandwidth.

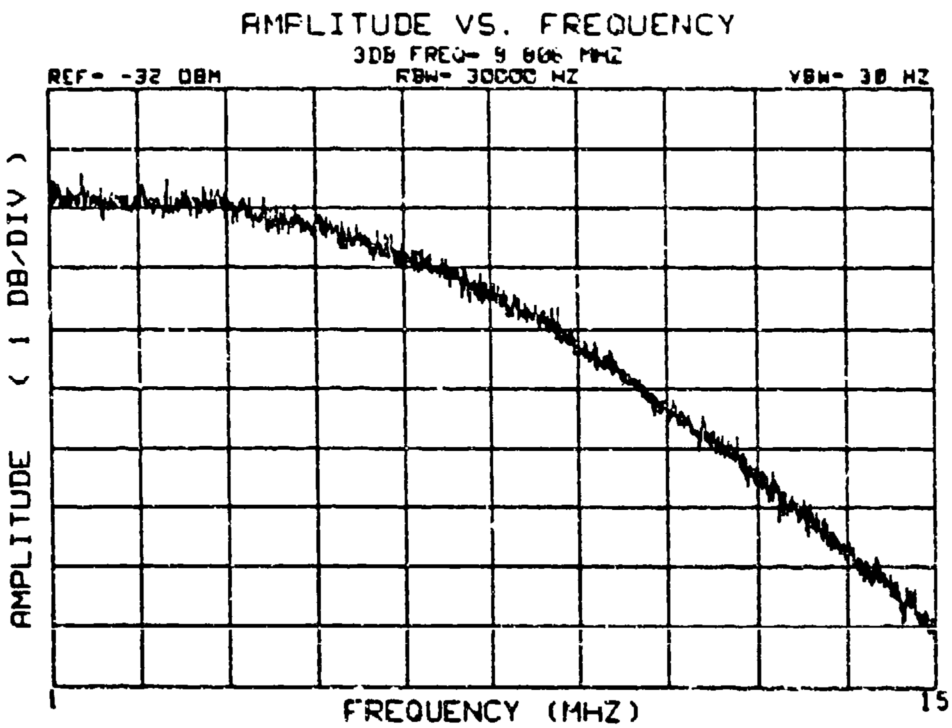

FIGURE A-3. Spectrum Analyzer Display Showing Frequency Response of Detector Video-Amplifier Chain.

Appendix B

GAUSSIAN OR RAYLEIGH DISTRIBUTION?

How can one tell whether the video output of an envelope detector system contains Gaussian- or Rayleigh-distributed noise? A very simple test can be performed with an oscilloscope. The most important difference between Gaussian- and Rayleigh-distributed noise is that Gaussian noise has a symmetrical amplitude distribution and Rayleigh noise is very asymmetrical.

To check the symmetry of the noise at the video output, the following steps should be carried out:

1. Set the oscilloscope trigger to trigger off the noise itself.

2. Set the triggering slope to positive.

3. Adjust the time/division and triggering level to obtain a trace that is just barely triggering the sweep and a positive-going noise "pulse" that is displayed on the screen (see Figure B-1). Measure the approximate amplitude of the noise pulse.

4. Set the triggering slope to negative and repeat step 3 to obtain a negative-going pulse. Measure the approximate amplitude of the noise pulse.

5. Calculate the ratio of the positive-to-negative noise pulses.

The ratio of the positive-noise pulse amplitude to the negative-noise pulse amplitude gives an indication as to the type of amplitude distribution of the video output noise. If the ratio is approximately 1, then the noise is probably Gaussian in nature. If the ratio is greater than 1.5 to 2.0, then the noise is Rayleigh-distributed. The greater the ratio, the more Rayleigh-distributed the noise.

Figures B-1 through B-5 are oscilloscope photos of Gaussian- and Rayleigh-distributed noise obtained using the above technique. Figures B-6 and B-7 are oscilloscope displays of each type of noise that show that even without using this technique a visual difference is evident.

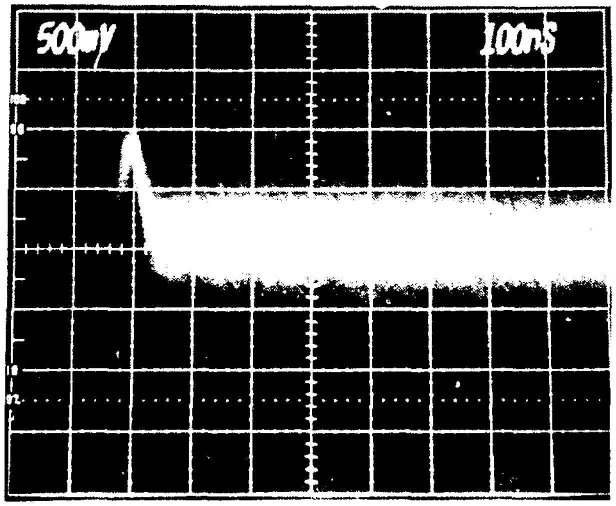

FIGURE B-1. Oscilloscope Display of a Noise Pulse.

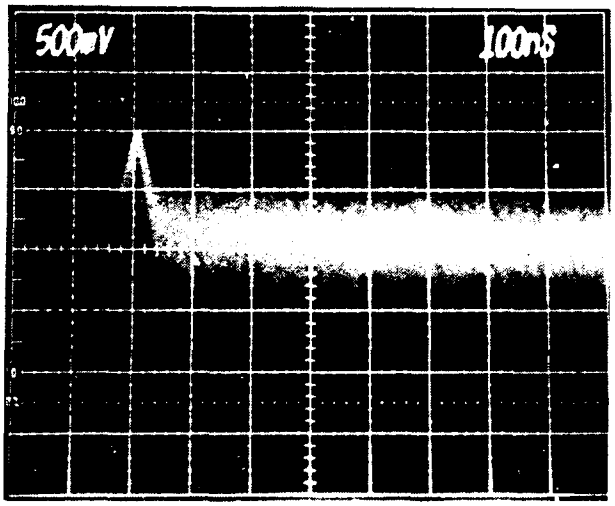

FIGURE B-2. Positive-Going Noise Pulse of Gaussian-Distributed Noise.

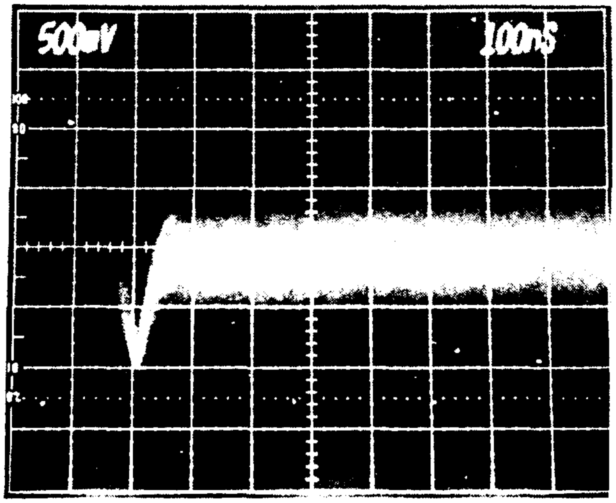

FIGURE B-3. Positive-Going Noise Pulse of Gaussian-Distributed Noise.

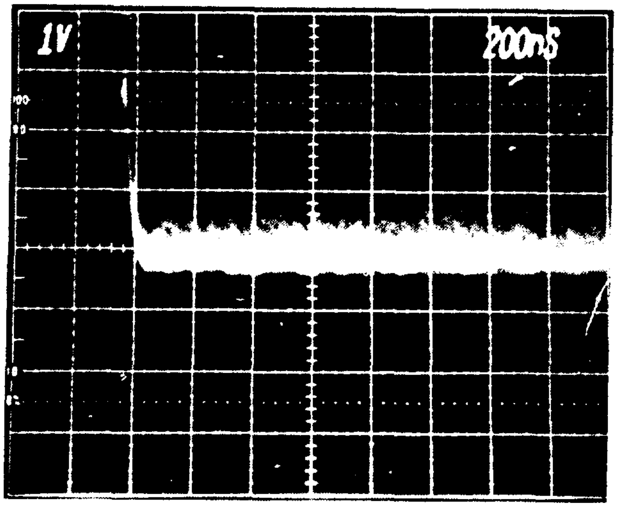

FIGURE B-4. Negative-Going Noise Pulse of Rayleigh-Distributed Noise.

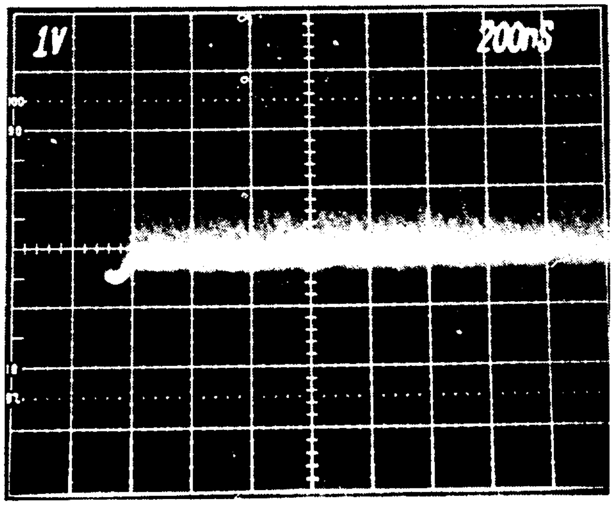

FIGURE B-5. Positive-Going Noise Pulse of Rayleigh-Distributed Noise.

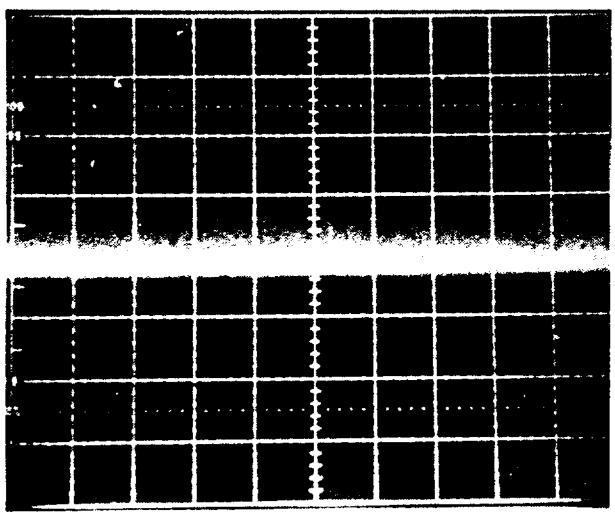

FIGURE B-6. Rayleigh-Distributed Noise. Scale is 1 V/division, 200 ns/division.

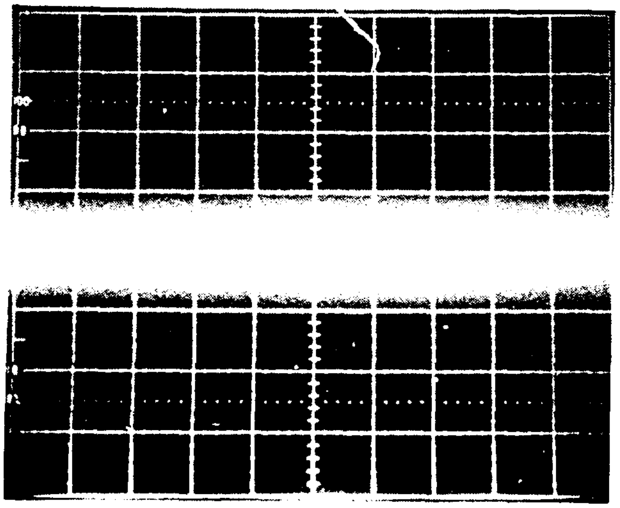

FIGURE B-7. Gaussian-Distributed Noise.
Scale is 500 mV/division, 100 ns/division.

REFERENCES AND BIBLIOGRAPHY

1. Lucas, W. J. "Tangential Sensitivity of a Detector Video System With RF Preamplification," *Proc. IEEE*, Vol. 113, No. 8, August 1966.

2. Schneider, Seymour. "Convert Specifications from Competing Noise Sources," *Microwaves and RF*, May 1987.

3. Schwartz, Mischa. *Information Transmission, Modulation, and Noise*. New York, McGraw-Hill, Inc., 1980. Pp. 377-401.

4. Hughes, Richard Smith. *Logarithmic Amplification*. Dedham, Mass., Aertech House, Inc., 1986. Pp. 4-13.

5. Lipsky, Stephen E. *Microwave Passive Direction Finding*. New York, John Wiley and Sons, 1987. P. 196.

Hughes, Richard Smith. *Determining Maximum Sensitivity and Optimum Maximum Gain for Detector Video Amplifiers With RF Preamplification*. China Lake, Calif., NWC, March 1985. (NWC TM 5352, publication UNCLASSIFIED.)

Mouw, R. B., and Schumacher, F. M. "Tunnel Diode Detectors," *Microwave Journal*, January 1966.

Skolnik, Merrill I., *Introduction to Radar Systems*, New York, McGraw-Hill, 1980.

Tsui, James Bao-yen. *Microwave Receivers With Electronic Warfare Applications*. New York, John Wiley and Sons.

INITIAL DISTRIBUTION

2 Naval Air Systems Command (AIR-5004)
2 Naval Sea Systems Command (SEA-09B312)
1 Commander in Chief, U. S. Pacific Fleet, Pearl Harbor (Code 325)
1 Commander, Third Fleet, San Francisco
1 Commander, Seventh Fleet, San Francisco
2 Naval Academy, Annapolis (Director of Research)
1 Naval War College, Newport
1 Air Force Intelligence Agency, Bolling Air Force Base (AFIA/INTAW, MAJ R. Esaw)
12 Defense Technical Information Center, Alexandria
1 American Electronic Laboratories, Incorporated, Lansdale, PA (J. Wadkowski)
2 California Microwave, Incorporated, Sunnyvale, CA
    R. Hardy (1)
    J. Hettinger (1)
3 Ford Aerospace and Communications Corporation, Newport Beach, CA
    S. Carruth (1)
    P. Juul (1)
    J. Possi (1)
1 Hudson Institute, Incorporated, Center for Naval Analyses, Alexandria, VA (Technical Library)